RSC Advances

REVIEW

View Article Online
View Journal | View Issue

Cite this: *RSC Adv.*, 2026, **16**, 25174

Recent advances of cyanine dyes in tumor theranostics: molecular modification, delivery strategies, and synergistic mechanisms

Dan Zhao,[c] Yaping Xiao,*[b] Mengyang Li *[a] and Liang Luo *[c]

The phototheranostic system has garnered significant attention due to its dual functionality of combining imaging and treatment. Moreover, while achieving non-invasive, real-time imaging and precise spatiotemporal controlled treatment, it also maintains low toxicity to normal tissues. Among the phototheranostic systems, cyanine dyes are a kind of ideal near-infrared (NIR) photosensitizer for phototheranostics. However, challenges still remain in terms of photostability, tumor selectivity, and diagnostic and treatment efficiency. This review summarizes advances of cyanine dye-based phototheranostics in tumor diagnosis and treatment over the past five years, with a focus on molecular modifications and nanostructure construction, delivery strategies, and synergistic mechanisms in integrated platforms for enhancing functionality. The review also looks ahead to future opportunities and challenges of cyanine dyes in tumor theranostics.

Received 3rd April 2026
Accepted 4th May 2026

DOI: 10.1039/d6ra02819e

rsc.li/rsc-advances

1. Introduction

Malignant tumors, characterized by invasive pathology originating from abnormal cell proliferation,[1] possess the ability to infiltrate adjacent tissues and metastasize *via* hematogenous[2,3] or lymphatic pathways.[4] As a result, they represent one of the most significant threats to global health.[5] Clinically, traditional diagnostic and therapeutic approaches are often administered separately, which complicates precise tumor localization, real-time treatment monitoring, and accurate prognosis assessment.[6] In the era of personalized oncology, researchers are redefining cancer management through integrated theranostics.[7,8] This precision medicine strategy synergizes diagnostics and therapeutics, allowing real-time monitoring of treatment progression, timely efficacy evaluation, and dynamic adjustment of therapeutic regimens.[9,10]

With advances in materials science and technology, various theranostic platforms activated by light,[11,12] ultrasound,[13] magnetic field[14,15] or radiation[16,17] have been developed. Among them, phototherapeutic systems that combine diagnostic imaging, particularly fluorescence and photoacoustic imaging (PAI), with phototherapy have garnered widespread attention for their multifunctional capabilities. In imaging diagnostics, fluorescence imaging (FLI) not only enables non-invasive, real-time, and high-resolution imaging,[6] but also simultaneously captures molecular signatures of tumor metabolism and microstructure.[18] Especially, photosensitizers activated by near-infrared (NIR) light can fully leverage the excellent tissue penetration capabilities of the light,[19,20] enabling diagnosis and treatment of deep-seated tumors. In contrast, PAI detects a phonon after light excitation, exceeding the optical diffusion limit and offering deeper tissue penetration.[21] In terms of therapy, spatiotemporal control of light enables precise localized treatment, thereby maximizing therapeutic efficacy while minimizing systemic toxicity.[22]

An ideal phototherapeutic agent must be able to differentiate tumors from healthy tissues through active or passive targeting. It also needs to generate detectable signals for diagnosis and release cytotoxic payloads for tumor ablation. Among them, cyanine dyes have come into our sight and garnered significant attention. They are a class of structurally tunable compounds composed of nitrogen-containing heterocycles linked by an odd-numbered polymethine chain terminating in a cationic nitrogen atom.[5] As a family of classical organic fluorescent dyes, cyanine dyes exhibit unique characteristics such as high molar absorption coefficients and narrow absorption/emission bands in the NIR region.[23,24] Through strategic modifications of the chain length and the introduction of electron-donating or electron-withdrawing substituents, their absorption and emission spectra can be precisely adjusted.[25–31] Additionally, the structural versatility of cyanine dyes enables flexile molecular engineering, supporting their decades-long biomedical application.[32–36] A typical clinical validation of this dye category is indocyanine green (ICG), the first NIR fluorescent dye

[a]*College of Chemistry & Pharmacy, Northwest A & F University, Yangling, Shaanxi, 712100, China. E-mail: myli@nwafu.edu.cn*

[b]*School of Life and Health Technology, Dongguan University of Technology, Dongguan, 523808, China. E-mail: 15982103680@163.com*

[c]*National Engineering Research Center for Nanomedicine, College of Life Science and Technology, Huazhong University of Science and Technology, Wuhan, 430074, China. E-mail: liangluo@hust.edu.cn*

approved by the US Food and Drug Administration (FDA).[37] In recent years, more and more properties of cyanine dyes have been discovered. Among the most important findings is that cyanine molecules can self-assemble into supramolecular structures such as H-aggregates or J-aggregates in different solutions and at different concentrations.[38,39] H-aggregates are arranged in parallel between molecules, exhibiting a blue shift in absorption peaks, while J-aggregates adopt a head-to-tail arrangement, showing a red shift in absorption peaks. By modulating the solution concentration, temperature, and solvent properties, the formation of these aggregates can be precisely controlled, enabling specific optical properties in different environments. Notably, cyanine aggregates demonstrate improved photostability and aggregation-induced phototherapy effects, making them highly promising agents for photothermal therapy (PTT) or photodynamic therapy (PDT).[38] Despite ongoing challenges in tumor selectivity, theranostic efficiency, and photostability, cyanine dyes continue to be actively investigated even after more than 60 years of use.

The structure characteristics, synthetic methods, optical properties, organic and inorganic nano-encapsulation, and biological applications of cyanine dyes for phototheranostics have been summarized in several reviews.[40–45] In this review, we focus on the advances of cyanine dyes in tumor theranostics over the past five years, presenting a new perspective that highlights strategies for enhancing tumor targeting and improving diagnostic and therapeutic functionality. Specifically, we emphasize delivery strategies based on biological modification and discuss the underlying mechanisms that enhance diagnostic and therapeutic performance (Fig. 1). The review concludes with an outlook on the opportunities and challenges associated with cyanine dyes in tumor theranostics.

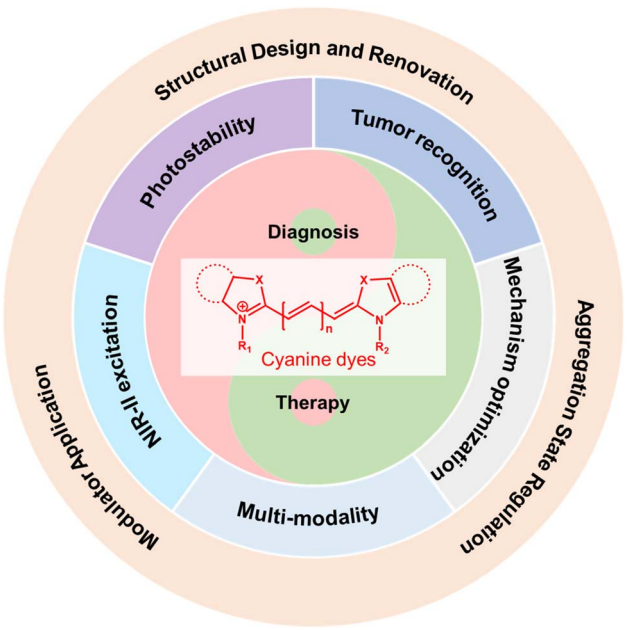

Fig. 1 Scheme of construction strategy for cyanine dye-based theranostics.

2. Tumor targeting and specific response theranostics

Effective tumor site identification and accumulation are prerequisites for the development of integrated theranostic agents. Although cyanine dyes possess inherent tumor-targeting properties, their accumulation efficiency remains insufficient to achieve precise tumor localization. To overcome this limitation, researchers have engineered cyanine dyes through targeted group modifications,[46,47] supramolecular assembly,[48] or nanocarrier encapsulation[49] to enhance their specificity for tumor recognition and accumulation. Additionally, the incorporation of stimulus-responsive annihilation moieties[50] or regulated dye aggregation states[51] to develop tumor-activated photosensitizers (PS) has greatly improved the precision of lesion-targeted diagnosis and treatment.

2.1. Passive targeting strategy

The pathological features of solid tumors, disrupted vasculature, enlarged endothelial gaps, and impaired lymphatic drainage, are collectively termed the enhanced permeability and retention (EPR) effect. This means that nanoscale drug carriers can more easily enter and remain at tumor sites.[52] By leveraging the EPR effect, tumor-selective drugs can simultaneously enhance diagnostic and therapeutic efficacy while reducing off-target toxicity. Nanoparticles with an appropriate size and surface charge can effectively evade endocytic clearance and maximize tumor accumulation. Encapsulation can be achieved through diverse approaches, including nanoparticle self-assembly, amphiphilic polymer encapsulation, and biocarrier-based strategies such as coating with serum albumin, tetrahedral framework nucleic acids (tFNAs), or bacterial membranes. These strategies improve probe water solubility and stability, reduce systemic clearance, prolong plasma half-life, and ultimately facilitate the construction of passively targeted nano-theranostic agents.

As a classic supramolecular characteristic of cyanine dyes, J-aggregation drives the spontaneous formation of structurally well-defined nanoparticles with highly arranged molecular packing.[53,54] This structural feature not only enhances the light-harvesting efficiency[55–57] and photostability[58,59] but also endows the dye with a favorable nanoscale size, thereby enabling passive tumor accumulation *via* the EPR effect. Therefore, the rational design of J-aggregates represents an effective strategy in dye chemistry to improve the *in vivo* performance of cyanine-based theranostic systems. Recently, Peng *et al.*[60] reported a strategy that utilizes the inherent surface charge of a Cyanine PS, 4-((*E*)-3-((*E*)-5-iodo-1,3,3-trimethylindolin-2-ylidene)prop-1-en-1-yl)-1-methylquinolin-1-ium iodide (IDMQ), to induce J-aggregation and drive their spontaneous self-assembly into nanoparticles (Fig. 2A). Leveraging the EPR effect typical of solid tumors, this approach achieved over a 10-fold enhancement in tumor site fluorescence imaging while using only twice the dye dose (Fig. 2B). Furthermore, negligible fluorescence signals were detected in off-target organs such as the colon, lungs, heart, spleen, and liver (Fig. 2C and D).

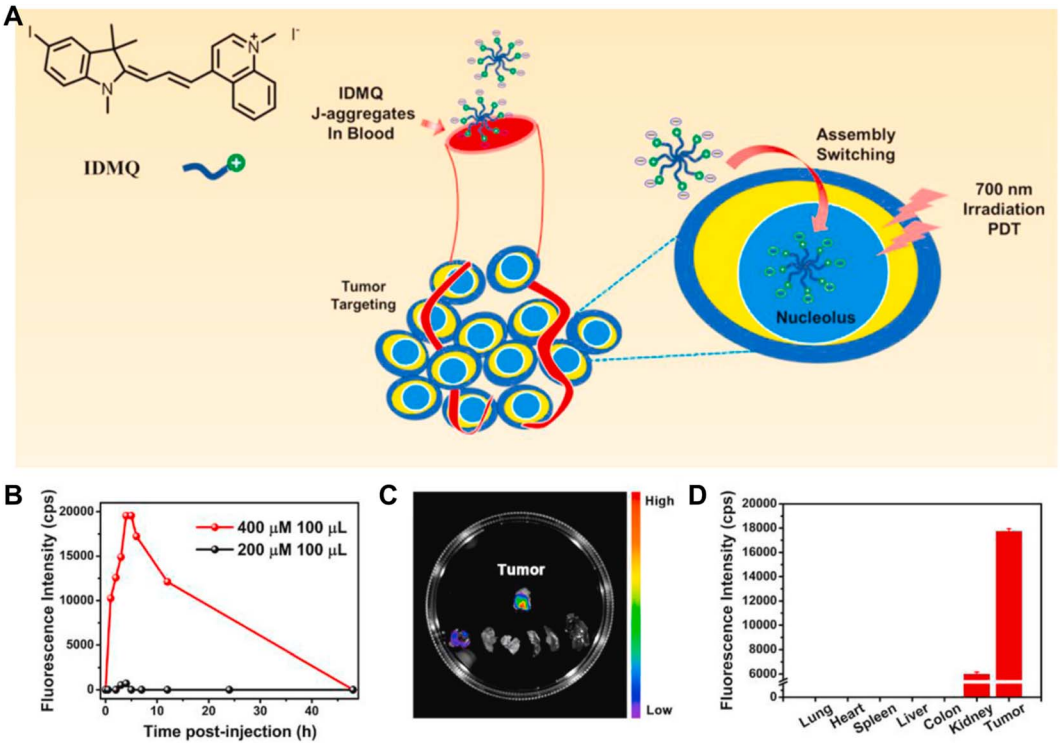

Fig. 2 (A) Chemical structures of free IDMQ and IDMQ J-aggregates and their smart J-aggregates system targeting tumors for PDT. (B) Fluorescence intensity changes of the murine tumor with time. (C) Fluorescence imaging (from top to bottom, left to right: tumor, kidney, colon, lung, heart, spleen, and liver) and (D) fluorescence intensity of various organs at 4 h after IDMQ injection (tail vein injection, 400 μM, 100 μL, 1.73 mg kg^{-1}). Reprinted with permission from ref. 60, copyright 2020 Elsevier.

Albumin, as a major serum protein, has demonstrated considerable potential in drug delivery. Its inherent biocompatibility, low immunogenicity, and natural ability make it an ideal vehicle for drug delivery.[20,61–63] Yu *et al.*[64] innovatively proposed an *in vivo* self-assembly of albumin and PS. This approach involved synthesizing a C8 heptamethine cyanine PS featuring dual *N*-alkyl chains with a total carbon chain length of eight atoms. Upon intravenous administration, the compound rapidly and efficiently self-assembled with endogenous serum proteins to form nanoscale dye–albumin complexes. By leveraging endogenous serum transport, the C8 complex achieved markedly prolonged circulation time and enhanced tumor-specific accumulation.

tFNAs are self-assembled from four equimolar concentrations of single-stranded nucleic acids with equal length.[65,66] Based on this, tFNAs can be precisely controlled in size and geometric shape with a simplified preparation process. More importantly, compared to traditional nucleic acids that are prone to degradation, tFNAs constructed *via* DNA origami technology showed exceptional dispersibility and stability. Additionally, the nanotetrahedral structure endows tFNAs with strong mechanical strength and inherent cell membrane permeability. Thereby, tFNAs can significantly enhance the dispersion and photostability of cyanine dyes in therapeutic and diagnostic applications. Recently, Li *et al.*[65] utilized this aptamer-tFNA delivery system to deliver Cy5 and achieved its sustained retention in tumors. Besides, Meng *et al.*[66] employed tetrads DNA to directly encapsulate hydrophobic cyanine dye IR780 through π–π stacking and electrostatic interactions. This strategy significantly improved water solubility and extended the blood circulation half-life from less than 3 h to 15 h. The tetrads DNA-IR780 complex achieved enhanced tumor accumulation and more efficient phototherapy of tumors.

Bacteria, intrinsically linked to human health and disease pathogenesis, possess the ability to actively sense dynamic environmental signals and migrate toward specific sites. These intrinsic properties establish them as a promising platform for targeted biomedical delivery.[67] For instance, Wang[68] employed *Escherichia coli* as a carrier to deliver theranostic agents to chemotherapy-resistant tumors *via* electrostatic adsorption and bioorthogonal click chemistry. This bacterial–drug complex effectively circumvented multidrug resistance mechanisms by evading the efflux pump, offering a novel strategy for chemotherapy-resistant tumors. Beyond their role as passive carriers, the inherent immunogenicity of bacteria also holds great potential for practical applications. With appropriate modification, bacteria can function as immunepotentiators, effectively enhancing the body's immune response and thereby significantly improving the efficacy of anticancer therapies. Sun *et al.*[69] demonstrated this by exploiting the hypoxia-directed tropism of the Salmonella VNP20009 to deliver the photosensitizer N782 to tumor tissue for PDT. The synergistic effect of bacterial immunogenicity and phototherapy effectively triggered the release of tumor antigens. It also downregulated

Table 1 Target functionalized theranostics[a]

Target	Cy dyes	Increased fluorescence intensity	Enhanced therapeutic effect	References
The L1 cell adhesion molecule (L1CAM)	Ap-β-gal-Fret	—	—	46
BRD4	PTJQ	—	—	47
Osteosarcoma	Cy7-TCF-PEG-TPPRVPLLTFGS	2.04	—	52
Programmed cell death protein 1	a-PD-1-DBCO	24	—	63
Folate receptor	LET-I-FA	—	—	70
Epidermal growth factor receptor	Pan-Hcy	3.5	7.1	71
Human epidermal growth	MMAE-Cy5-trastuzumab	—	—	72
factor receptor 2	Trastuzumab-mI2XCy-Ac	2	—	73
C–X–C motif chemokine receptor 4	Cy5-1S-FC131	—	—	75
$\alpha_v\beta_3$-integrin	Cy5.5-c[RGDKLAK]	—	2.82–3.24	76
	IR-PEG-cRGD	4.79		79
Man receptor	SeBDP@TPZ-S-S-Cy/Man NPs	~1.6	—	77
Estrogen receptor α	FAPI-Cy7-Cl	4.5	—	80
CD133	CD133Ab-grafted Cy5.5/ PFOB@P-HVs	3	—	81
CD20	aCD20-mAB-P/ P-ibrutinib-Cy3.5	—	—	82
Poly ADP-ribose polymerase	Rib-MHI-148	—	3	83
CD44 receptor	IR783-Fe@MnO_2-HA	—	—	84
Mcl-1 protein	Nap	—	—	85
Biotin acceptor	T-BNCy5	—	>9	86
Asialoglycoprotein receptor	PIR NPs	>2.0	—	87
Transferrin receptor	Tf-IRLy NPs	—	2.67 fold	88
Hypoxic	N–V–J	—	—	69
Tumor	LZ-1105@HAm	4.7	—	20
	IR820-TPE@B-Exo	—	—	78

[a] "—" date not reported or reported cannot be quantified.

programmed cell death ligand 1 (PD-L1) expression, an immune checkpoint molecule that suppresses T-cell function, thereby alleviating its immunosuppressive effect on T cells. These effects, driven by the combined action of tumor antigen-mediated immune cell recruitment and the relief of T cell immunosuppression, reshaped the tumor microenvironment. The state converted from a "cold tumor" with sparse immune cell infiltration and weak immune response, to a "hot tumor" featuring abundant immune cell infiltration and strong anti-tumor activity. Ultimately, this conversion elicited a systemic anti-tumor immune response.

2.2. Active targeting strategy

Compared with normal tissues, malignant tumors exhibit significant overexpression of tumor-specific receptors on their surfaces (such as folate receptor,[70] epidermal growth factor receptor,[71] and human epidermal growth factor receptor 2 (ref. 72 and 73)). This phenomenon is driven by epigenetic alterations, which sustain the uncontrolled proliferation, invasion, and survival of tumor cells, as well as their adaptation to the microenvironment. These overexpressed features, characterized by high abundance, surface accessibility, and essential roles in tumor biology, provide an ideal molecular basis for precise tumor identification and active targeting through ligand-receptor recognition. By functionalizing nanocarriers with targeting ligands such as antibodies,[73,74] peptides,[75,76] carbohydrates,[77] or vitamins,[78] tumor-specific binding and receptor-mediated endocytosis can be achieved, thereby enhancing theranostic precision and minimizing systemic side effects (Table 1).

2.2.1. Targeting group modification. The structural versatility of cyanine dyes enables the direct integration of targeting moieties into their scaffold, providing a straightforward strategy to confer active targeting for theranostics. This design facilitates specific recognition between the modified dye and receptors overexpressed on tumor cells, leading to preferential accumulation at tumor sites. Consequently, it enhances imaging specificity, improves signal-to-noise ratio, and supports safer, more efficient theranostic integration. Tang *et al.*[47] exemplified this approach by covalently conjugating JQ-1, a bromodomain protein 4 (BRD4) inhibitor, to a cyanine dye scaffold, thereby achieving selective recognition of BRD4—a key regulator of cell cycle and differentiation that is overexpressed in multiple types of tumor cells. Through specific interaction between the BRD4 inhibitor and the BRD4 bromodomain, the prepared photothermal agent achieved targeted binding, thereby prolonging tumor retention and significantly reducing off-target effects in normal tissues. Chen *et al.*[89] developed Crizotinib-IR808@BSA nanoparticles for NIR-II imaging-guided chemophototherapy in colorectal cancer. Crizotinib, which targets cellular-mesenchymal epithelial transition factor (c-Met, a tyrosine kinase receptor frequently overexpressed in tumors

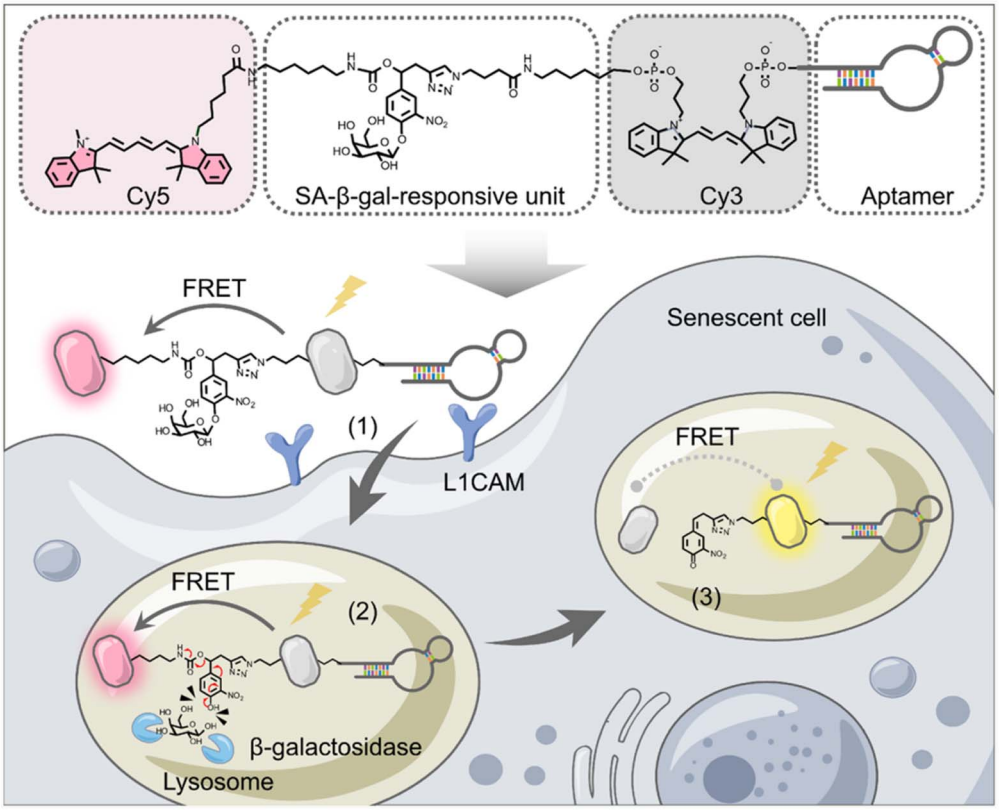

Fig. 3 Schematic illustration of the design of the aptamer conjugate-based ratiometric fluorescent probe and the underlying recognition and responsive mechanisms toward therapy-induced cancer senescence. Reprinted with permission from ref. 46, copyright 2024 American Chemical Society.

and critical for tumorigenesis), was covalently conjugated to the near-infrared dye IR808. Further bovine serum albumin (BSA) encapsulation was employed to enhance optical stability and water solubility. Benefiting from the combined effect of passive and active targeting, the nanoparticles exhibited a blood half-life of 24.23 minutes, representing an over 8-fold increase compared to free ICG (180 seconds). The system achieved a high tumor inhibition rate of 96% and enabled high-contrast NIR-II imaging of tumor vasculature, with a signal-to-background ratio of 1.29.

Aptamers are short-stranded oligonucleotides typically composed of 20 to 100 nucleotides, featuring a unique tertiary structure that enables them to specifically recognize target biomarkers. Therefore, designing drugs with specific aptamers as tumor-targeting moieties holds great potential for enhancing tumor recognition efficiency. Based on this, Liu *et al.*[46] developed an aptamer conjugate-based ratiometric cyanine probe for precise imaging of therapy induced cancer senescence, by leveraging the aptamer-mediated L1CAM recognition. As shown in Fig. 3, this aptamer-modified probe can precisely identify and internalize senescent cancer cells. Subsequently, the elimination of Förster resonance energy transfer between two cyanine dyes induced by lysosomal senescence-associated β-galactosidase (SA-β-gal) triggers ratiometric fluorescence changes, enabling precise localization and high-contrast imaging of senescent cells.

Antibodies are immunoglobulins capable of specific antigen binding. By leveraging this selective recognition, monoclonal antibodies (mAbs) can be conjugated with diagnostic or therapeutic payloads to form antibody–drug conjugates (ADCs).[73,74] ADCs harness the high affinity and precision of mAbs for tumor-associated antigens, enabling targeted localization of drug cargoes within cancer cells and promoting their selective accumulation. Moreover, through tumor-microenvironment-responsive release mechanisms, systemic toxicity to healthy tissues can be minimized.[90] When challenges such as labeling efficiency and cargo aggregation are effectively addressed, ADCs can substantially enhance the precision of tumor eradication guided by diagnostic imaging.[71]

2.2.2. Biocarrier encapsulation. Beyond direct conjugation of targeting groups to photosensitizers, encapsulating probes within ligand-functionalized nanocarriers offers an alternative and effective targeting strategy. This method combines passive and active targeting mechanisms to improve the delivery of theranostic agents to tumors. Various synthetic nanocarriers, including targeted micelles, liposomes, and inorganic nanoparticles, have been shown to extend blood circulation half-life and enhance tumor accumulation in numerous studies.[81,88] Nevertheless, as exogenous materials, most synthetic nanocarriers remain prone to rapid immune clearance, which still limits their overall accumulation efficiency in tumors. In stark contrast, biologically derived carriers, including certain

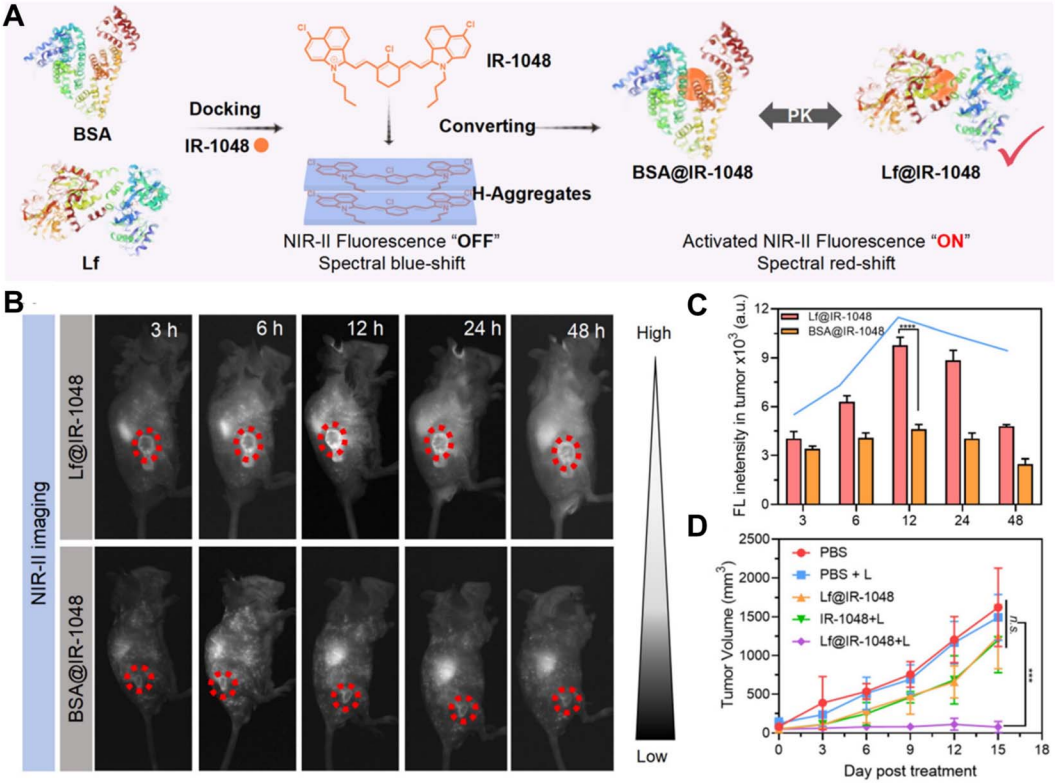

Fig. 4 (A) The synthesis process of Lf with BSA proteins hitchhiking IR-1048. (B) Time-dependent *in vivo* NIR-II fluorescence imaging of CT26 tumor-bearing mice after the intravenous injection of BSA@IR-1048 and Lf@IR-1048 (IR-1048: 2 mg kg^{-1}) under excitation wavelength of 980 nm. (C) Corresponding fluorescence intensity of tumor sites at different time points. (D) Tumor growth curve of mice with various treatments. Reprinted with permission from ref. 92, copyright 2024 Ivyspring.

proteins, cell membranes, and exosome camouflage, offer distinct advantages for targeted drug delivery. Their biomimetic nature not only endows them with improved biocompatibility and enhanced immune escape capability, but also provides them with tumor targeting ability.[91]

Protein-based carriers enable the delivery of therapeutic cargo by virtue of their excellent biocompatibility and low immunogenicity. Moreover, protein–dye interactions can modulate fluorophore conformation and aggregation, suppress non-radiative transitions from molecular rotation and vibration, and thereby tune dye photophysical properties. Compared to serum proteins, which mediate passive targeting *via* the EPR effect, active targeting proteins demonstrate greater advantages in both tumor targeting and molecular optical properties regulation. Jiang *et al.*[92] pioneered the application of physiological lactoferrin (Lf) for theranostic delivery (Fig. 4A). A systematic comparison between Lf and BSA conjugates with the NIR-II dye IR-1048 revealed the critical advantages of the Lf system. Structurally, Lf@IR-1048 demonstrated a stronger binding affinity (-10.83 kcal mol^{-1}) than its BSA counterpart, leading to a >100% enhancement in NIR-II fluorescence brightness (Fig. 4B and C). Mechanistically, unlike the passive accumulation of BSA@IR-1048, Lf@IR-1048 achieved active targeting *via* receptor-mediated endocytosis, which is driven by the specific recognition of Lf receptors overexpressed on tumor cells. Functionally, this significantly enhanced tumor accumulation enabled Lf@IR-1048 to achieve 94.8% tumor growth inhibition under NIR-II phototherapy, representing a substantial improvement over control groups (Fig. 4D).

Biologically derived carriers, particularly exosomes[78] and cell membranes,[20,93] offered superior biocompatibility and immune evasion capabilities compared to synthetic counterparts. Crucially, the retained biomolecular components, such as exosomal integrins and tumor cell membrane homotypic binding proteins, enable active targeted recognition.[94] This dual functionality synergistically enhances lesion-specific accumulation while avoiding immune clearance.[95] Huang *et al.*[20] exemplified this paradigm by employing tumor cell membrane-encapsulated theranostic agents (Fig. 5A). Assembly of cyanine dye-serum albumin complexes and subsequent tumor-derived membrane coating yielded biomimetic nanoparticles with a 3.0-fold longer plasma half-life (1.92 h *vs.* 0.63 h for free dye) (Fig. 5B), attributed to membrane-mediated immune evasion. Leveraging homotypic targeting, the agent demonstrated significantly enhanced tumor accumulation, with photoacoustic and fluorescent signals increasing by 1.7-fold and 4.7-fold, respectively (Fig. 5C and D). Consequently, under 808 nm irradiation, robust photothermal efficacy was achieved, resulting in 100% tumor inhibition and complete tumor ablation compared to the control group (Fig. 5E).

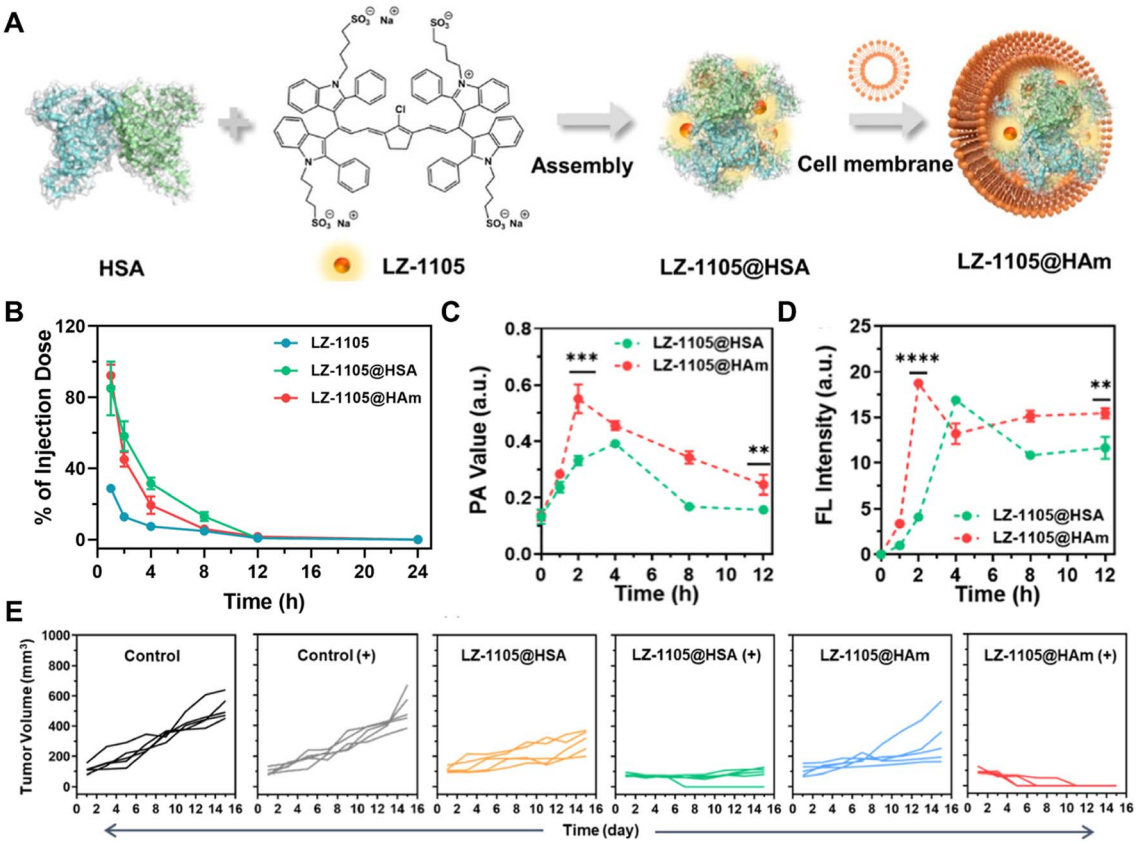

Fig. 5 (A) Preparation of homologous cell membrane-coated albumin-energized NIR-II cyanine dye (LZ-1105@HAm). (B) Pharmacokinetic curves of total LZ-1105 in blood from the mice. (C and D) Time-dependent PA (C) and FL (D) intensity. (E) Tumor growth curves of the mouse after different treatments. Reprinted with permission from ref. 20, copyright 2025 American Chemical Society.

2.3. Tumor microenvironment responsive theranostics

The development of targeted theranostic agents aimed to improve the diagnostic accuracy and therapeutic efficiency of drugs. However, a series of challenges persists, including non-specific recognition during diagnosis[96] and phototoxicity in normal tissues caused by constitutively active agents.[97] To address these challenges, activatable theranostic agents have been developed that leverage distinctive tumor microenvironmental features, such as hypoxia,[32,49,98–100] acidity,[70,85,101,102] and overexpressed enzymes.[46,50,51,73,96] These agents remain biologically inert during systemic circulation, and are selectively activated only upon exposure to tumor-specific stimuli, enabling precise imaging and therapeutic functions. Cyanine dyes exemplify this approach through two responsive activation mechanisms. The first approach involves conjugating them to tumor microenvironment-sensitive quenching groups *via* stimuli-cleavable linkers (*e.g.*, enzyme-, pH-, glutathione-, or ROS-responsive bonds). This design restrains their photoactivity until tumor-specific stimuli trigger linker cleavage or structural rearrangement, thereby recovering fluorescence and phototherapeutic function (Fig. 6). Based on this paradigm, diverse activatable photosensitizers responsive to various tumor microenvironmental cues have been developed (Table 2).

The second approach leverages their inherent aggregation-induced quenching in aqueous environments. In this case,

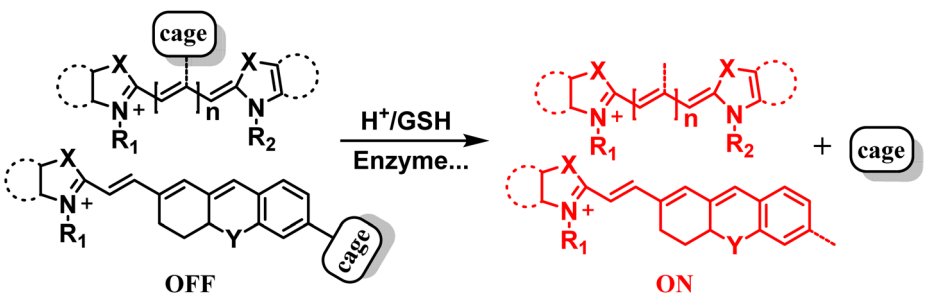

Fig. 6 Commonly used design strategies in constructing activatable cyanine dye-based theranostics.

Table 2 Tumor microenvironment-activated photosensitizers[a]

Stimuli	Responsive moiety	Cy dyes	Effect	References
Hypoxia	Azo bond	HDIM	—	32
	Nitrobenzene	CNO	—	49
	Nitrobenzene	BPN2	11.7-Fold FL	98
	Nitrobenzene	CyI-Cbl-NTR	Photocytotoxicity index 3.29	99
β-Galactosidase	β-Galactose	Ap-β-gal-Fret	Signal change 3-fold	46
Aldehyde dehydrogenase	Xenobiotic aldehyde	PS-CHO	—	50
Granzyme B (GraB)	Ile-Glu-Pro-Asp	Cy5.5-CBT-dimer	3.1-Fold FL enhancement	51
pH	Tertiary amine group	LET-I-FA	Ratio of FLT/N = 2.5 PA ratio of PAT/N = 4	70
	Tertiary amines	FPZ	PCE up to 69.96%	101
	Tertiary amines	Cy-Nap	—	85
	Molecular rearrangement	Cy-TPA	Signal-to-background ratio 6.4	102
Esterase	Acetyl (Ac)	Ab-mI2XCy-Ac	τ1/2 3.7-fold slower	73
Alkaline phosphatase (ALP)	Phosphate group	ALPIN-6I	Over 2000-fold enrichment	96
Glutathione	2,4-Dinitrobenzenesulfonate (DNBS)	Cyl-DNBS	6-Fold inhibition	97
	Quinone	Cy-Res	80-Fold FL enhancement	105
	3,5-bis(Trifluoromethyl) benzenethiol	CyI-S-diCF3	—	106
ROS	Thioketal linkage (TK)	DON-TK-BM	τ1/2 31.8 min	103
Oxidized BSA	3,5-Dioxocyclohexanecarboxylic acid (DHCA)	DIR	≈28-fold to background	104

[a] "—" date not reported or reported cannot be quantified.

disrupting their aggregated state using tumor-specific stimuli can also achieve responsive "on-off" switching for imaging and therapeutic applications. Lee *et al.*[107] engineered ammonium octasulfate anions as an intraluminal precipitant to construct liposomes with Cy5.5 encapsulation efficiency approaching 100%. Sulfonate-induced nano-precipitation confined Cy5.5 within self-quenched H-aggregates, achieving 98% fluorescence quenching. Upon liposomal disintegration, the complete dye was released and disaggregated from aggregates, restoring and enhancing fluorescence intensity by 60-100-fold (Fig. 7).

Liang *et al.*[51] synthesized enzyme-responsive chimeric nanoparticles *via* a reduction-instructed 2-cyanobenzothiazole (CBT)-Cys click condensation reaction (Fig. 8A). The resulting cyclic dimer CY5.5-CBT-Dimer spontaneously assembled into nanoparticles (Cy5.5-CBT-NPs) *via* hydrophobic interactions and π–π stacking, forming H-aggregates and inducing double fluorescence quenching through exciton coupling. However, after cell internalization, granzyme B (GraB) rapidly hydrolyzed the nanoparticle scaffold, triggering its disassembly and subsequent fluorescence activation (3.1-fold enhancement *in vivo*) (Fig. 8B). Since GraB activity was directly correlated with cytotoxic T lymphocyte (CTL) effector function in immune-mediated tumor killing, these nanoparticles could also serve as a real-time reporter of CTL activity. In a mouse model bearing B16-OVA melanoma, fluorescence activation of nanoparticle synchronously occurred with enhanced tumor infiltration of $CD8^+$ CTL during S-(2-boronoethyl)-L-cysteine hydrochloride-mediated tumor immunotherapy (Fig. 8C).

3. Strategies to enhance diagnostic and therapeutic capabilities

The preceding sections have outlined numerous strategies to enhance the targeting precision and stimulus-responsive switching of theranostic agents. These strategies primarily focused on improving targeting recognition capabilities, with limited attention given to critical limiting factors such as biological stability and tissue penetration depth.[108] This section will focus on the latest advances across four interconnected domains: molecular stabilization strategies, construction of NIR-II probes, engineered architectures with amplified theranostic outputs, and multimodal synergistic platforms with integrated complementary diagnostic and therapeutic modalities.

3.1. Molecular stability enhancement

The photostability of cyanine dyes is critically important, as it directly impacts the reliability, accuracy, and quality of data obtained from imaging and detection. Traditional cyanine dyes exhibit poor chemostability and photostability, which worsen as the polymethine chain lengthens. On one hand, the low steric hindrance around the polymethine chain makes it susceptible to attack by nucleophiles. On the other hand, the dense electron distribution along the chain renders it vulnerable to oxidants. In particular, singlet oxygen ($^1O_2$) generated by photoexcitation of the dye can oxidize the electron-rich polymethane chain,

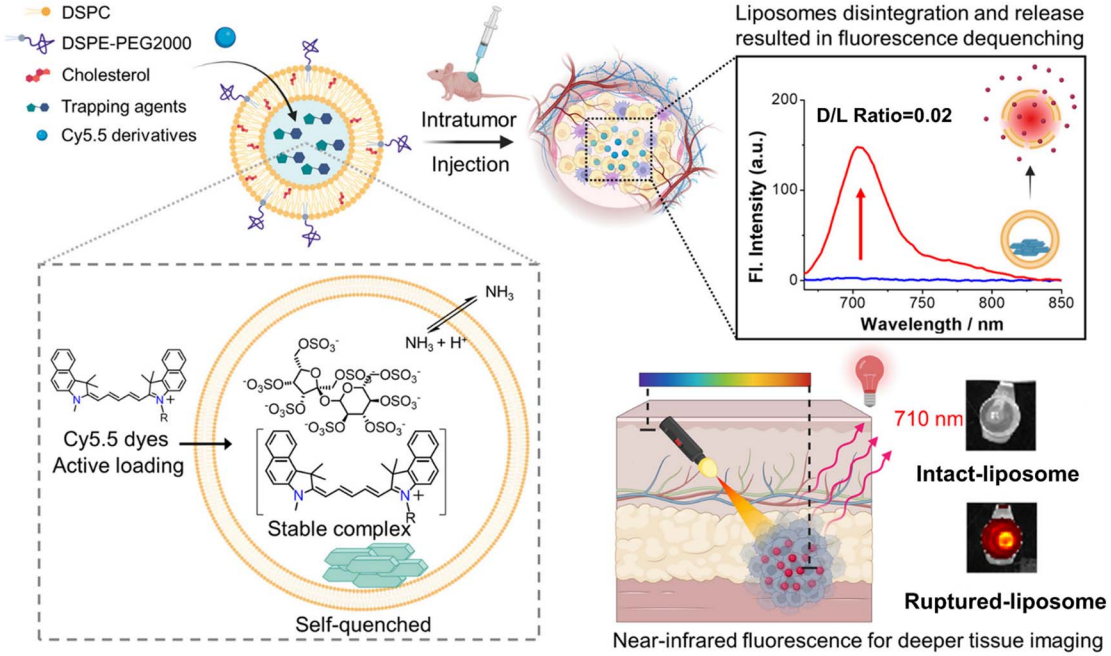

Fig. 7 Schematic illustration of the self-quenched Cy5.5-loaded liposomes for significant fluorescence enhancement with an excellent signal-to-noise ratio. Reprinted with permission from ref. 107, copyright 2024 Royal Society of Chemistry.

inducing irreversible photodegradation and consequent fluorescence reduction.[40,109]

Structure modification or utilizing them in a protective chemical environment are effective strategies for enhancing cyanine photostability. Introducing a five- or six-membered ring into the central position of heptamethine cyanine dyes, or introducing electron-deficient units into the cyanine framework to alter electron distribution, are two strategies to improve photostability.[40,110] Furthermore, introducing steric hindrance groups can also reinforce structural integrity by limiting nucleophilic attack. Smith's group pioneered molecular constraint strategies to stabilize cyanine dyes by isolating intermolecular interactions.[108,111–113] Their recent "double-constrained" molecular design addressed the vulnerability of the C4′-*O*-aryl bond in traditional cyanine to nucleophilic attack (Fig. 9A).[108] Specifically, this structure shielded the C4′-*O*-aryl bond through steric shielding, thereby protecting it from attack by biological nucleophiles. Additionally, the dye molecules maintained a distance of approximately 9 Å, thereby avoiding π-stacking-induced fluorescence quenching. The dye maintained structural integrity for 10 hours (Fig. 9B) when co-incubated with nucleophilic GSH (1 mM, room temperature), showing excellent stability compared to the unmodified control group. When it was conjugated to antibodies, the "double-constrained" design also prevented surface dye aggregation (Fig. 9C), achieving sustained tumor-to-background ratios exceeding 8 in murine xenografts at 72 h post-injection (Fig. 9D and E).

Protein- or nucleic acid-mediated structural stabilization and regulation could significantly enhance the photostability of cyanine dyes in aqueous solutions.[114] Additionally, regulating the aggregation state of the dyes, particularly the formation of J-aggregates[107,115] can further modulate stability[116] through exciton delocalized energy dissipation and oxygen scavenging effects. Cyanine molecules in the J-aggregate adopt an ordered head-to-tail arrangement with a slip-stacked conformation, forming a one-dimensional coherent exciton band. This configuration enables rapid exciton delocalization and non-radiative relaxation. As a result, the generation of $^1O_2$ is suppressed, fundamentally inhibiting excited-state-induced photooxidative degradation. In addition, the dense and ordered supramolecular stacking of J-aggregates effectively impedes the penetration of reactive species such as oxygen and solvent molecules. This minimizes the contact area between the dye and oxygen, further suppressing photooxidation. Through these two synergistic mechanisms, the rates of photobleaching and photodegradation of phthalocyanine dyes are substantially reduced, thereby enhancing their photostability. Peng *et al.*[117] developed J-aggregates (C5T-ET) through electrostatic co-assembly of cationic C5TNa and anionic Cy-Et to promote intermolecular close packing and induce intermolecular charge transfer (ICT). This strategy triggered ultrafast energy transfer, reducing the excited state lifetimes from hundreds of picoseconds (≈400 ps) to tens of picoseconds (≈22 ps). In addition, photodegradation was suppressed under 730 nm laser irradiation (0.1 W cm^{-2}), thereby enhancing the photostability of the dyes.

3.2. Constructing NIR II theranostics agents

As near-infrared fluorophores, cyanine dyes offer superior tissue penetration depth compared to visible-light fluorescent dyes. However, the excitation wavelengths of most cyanine dyes

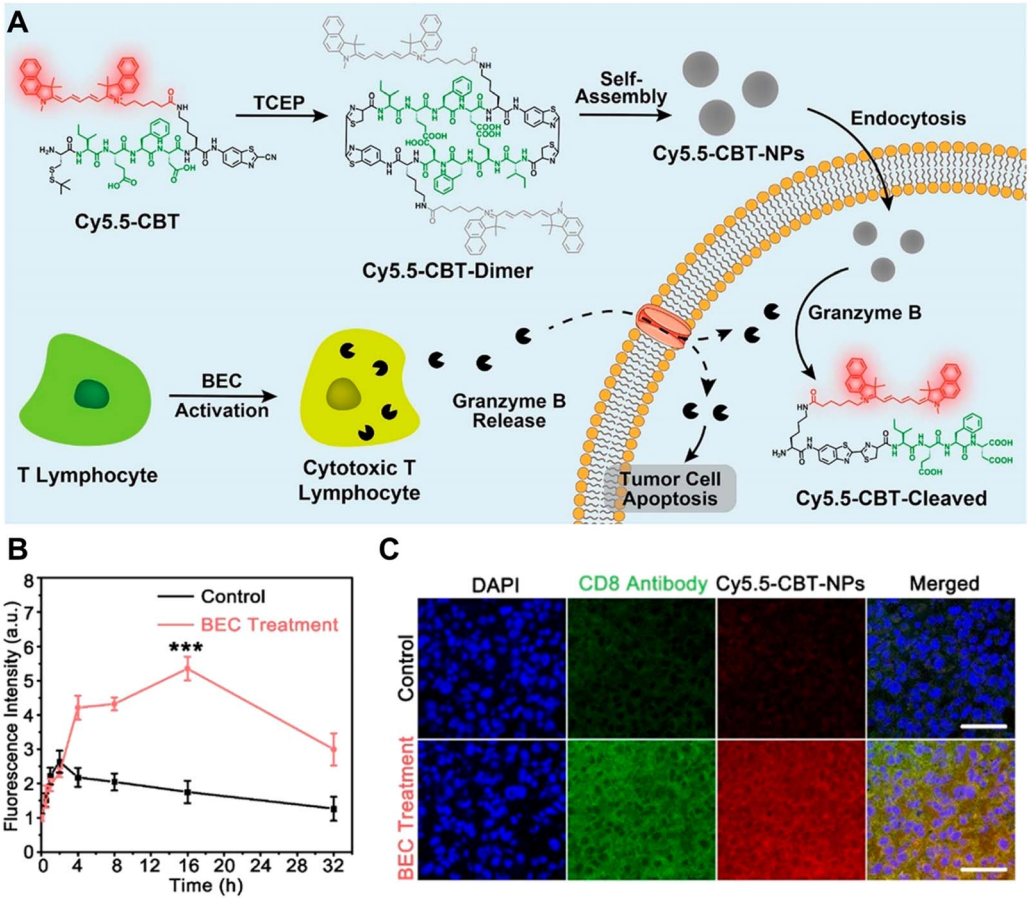

Fig. 8 (A) Schematic illustration of fluorescence-"dual quenched" Cy5.5-CBT-NPs preparation and cartoon representation of using Cy5.5-CBT-NPs to image the tumoricidal activity of cytotoxic T lymphocytes. (B) Time-dependent fluorescence intensity of the tumor after pretreatment with saline and Cy5.5-CBT-NPs. (C) Confocal fluorescence microscopy images of CD8 staining of tumor tissues. Reprinted with permission from ref. 51, copyright 2022 American Chemical Society.

fall within the NIR-I region (700–950 nm), which limits their *in vivo* applications due to the restricted tissue penetration depth of such excitation light. NIR-II (1000–1700 nm) radiation enables deeper tissue penetration compared to NIR-I light,[118] thereby enhancing imaging resolution, contrast, and therapeutic efficacy.[119] More importantly, biological tissues exhibit higher biological tolerance to NIR-II wavelengths. For example, the maximum permissible exposure for skin at 1064 nm (NIR-II, 1.0 W cm^{-2}) is three times that at 808 nm (NIR-I, 0.33 W cm^{-2}).[120] This expanded safety threshold enables NIR-II irradiation to utilize higher excitation power densities. Therefore, developing cyanine-based photosensitizers tailored for the NIR-II wavelength band represents a strategic approach to advance phototheranostic technologies.

Extending π-conjugation and incorporating strong donor/acceptor groups represent effective approaches to achieve a bathochromic shift in cyanine dyes, as they enhance the charge-transfer character and lower the HOMO–LUMO energy gap. Based on this principle, Wang group[121] introduced an electron-donating methoxyphenyl group at the terminal position of the cyanine dye, yielding YN-Glu. This modification expanded the conjugated system and increased the electron density of the dye molecule, thus extending the emission wavelength up to 1300 nm. Zhang *et al.*[122] synthesized a series of NIR-II heptamethine cyanines, NIR-ACs, through a simple ectopic substitution of the electron-donating amino group in Flav7 (Fig. 10A). This modification achieved the HOMO–LUMO separation and significantly extended the wavelength of symmetrical cyanine into the NIR-II region (Fig. 10B).

Modulating the aggregation state of cyanine dyes, particularly by alleviating H-aggregate or promoting J-aggregate formation, offers another effective strategy to redshift their absorption into the NIR-II window. The orderly arrangement facilitates constructive coupling of transition dipoles, leading to red-shifted absorption wavelengths with increased molar extinction coefficients, and altered fluorescence properties.[120] Lin and colleagues[123] developed a metal ion-assisted strategy to assemble cyanine dye IR1064 by exploiting the coordination interactions between them. Introducing different metal ions into the IR-1064 solution effectively regulated molecular arrangement through ion-specific coordination interaction. Notably, gadolinium ions (Gd^{3+}) effectively alleviated π–π stacking of H-aggregates between dye molecules, thereby promoting the formation of stable nano-assemblies in aqueous media. The maximum excitation and emission wavelengths of these nano-assemblies were 962 nm and 1098 nm, respectively.

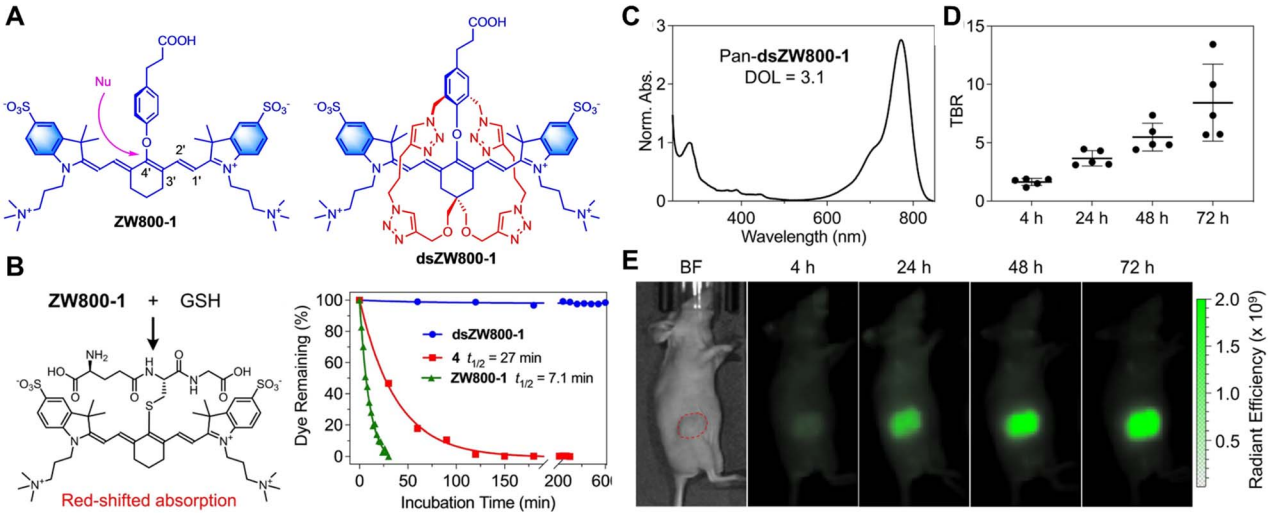

Fig. 9 (A) Introducing shielding arms to improve the stability of cyanine dyes. Nu: nucleophile. (B) Reaction of ZW800-1 with glutathione (GSH) to give a product with red-shifted absorption maxima band and comparison of dye stabilities in pH 7.4 PBS buffer with 1 mM GSH, room temperature. (C) Normalized absorption spectrum of Pan-dsZW800-1 (Degree of labeling, DOL = 3.1) in pH 7.2 PBS at room temperature. (D) Tumor-to-background ratio (TBR) from *in vivo* NIR-I imaging (ex: 745 ± 15 nm, em: 800 ± 10 nm) of JIMT-1 tumor-bearing mice ($N = 5$) after intravenous injection of Pan-dsZW800-1 (50 μg dose) and imaging at 4, 24, 48, and 72 h post-injection. (E) Representative *in vivo* NIR-I fluorescence images of the JIMT-1 tumor-bearing mice. Reprinted with permission from ref. 108, copyright 2023 Wiley.

3.3. Multimodal collaborative diagnosis and treatment

Phototherapy offers significant advantages such as minimal side effects and precise spatiotemporal control, yet its efficiency in single-modality applications remains limited. To overcome this challenge, a key research focus has been the development of phototherapeutic agents that integrate multimodal imaging with synergistic treatment modalities.

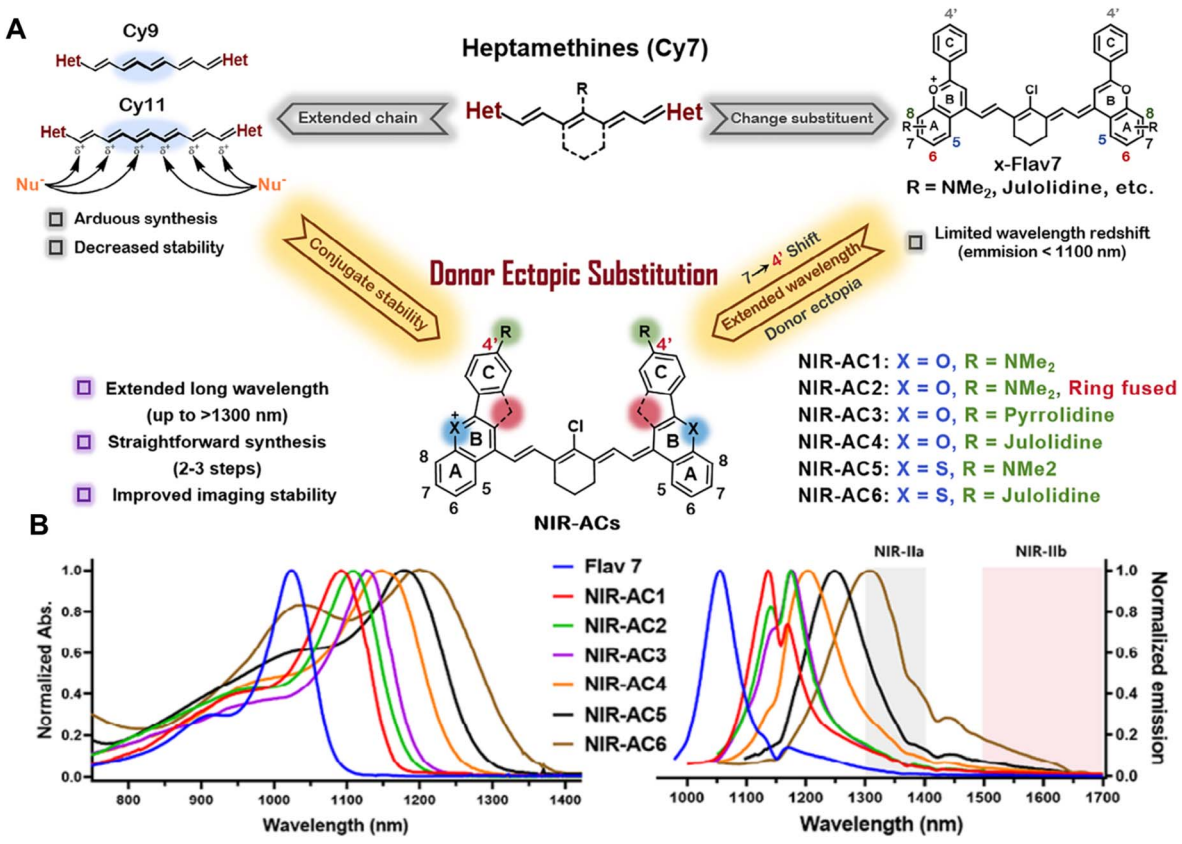

Fig. 10 (A) Donor ectopic substitution strategy guidance for constructing long-wavelength stable NIR-ACs dyes. (B) Absorption and emission spectra of Flav7 and NIR-ACs in DCM. Reprinted with permission from ref. 122, copyright 2025 Wiley.

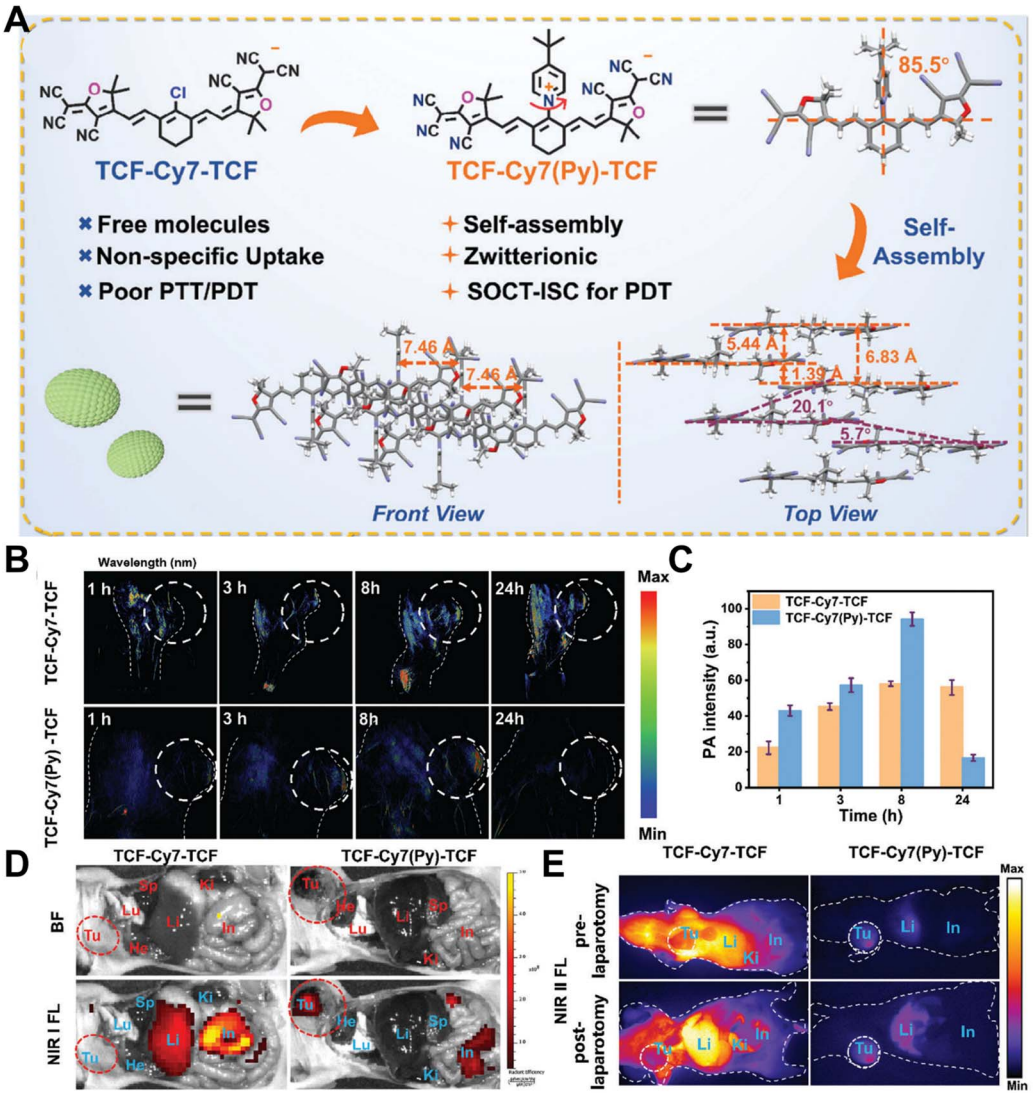

Fig. 11 (A) Schematic illustration of the self-assembly and stacking patterns of TCF-Cy7(Py)-TCF. (B) Time-dependent PAI of TCF-Cy7-TCF or TCF-Cy7(Py)-TCF in 4T1 tumor-bearing mice. The dashed circle indicates the tumor. (C) Relative PA intensities of tumor sites based on the quantitative analysis of (B). (D) NIR-I fluorescence images of surgically exposed tissues/organs. (E) NIR-II fluorescence images of tissues/organs before and after laparotomy. He: Heart; Li: liver; Sp: spleen; Lu: lung; Ki: kidney; In: intestine; Tu: tumor; FL: fluorescence; BF: bright field. Reprinted with permission from ref. 129, copyright 2024 Wiley.

3.3.1. Multimodal imaging. Multimodal diagnosis integrates complementary imaging methods, including FLI, PAI, magnetic resonance imaging (MRI), ultrasound imaging, positron emission tomography (PET), and others. Compared with single-modality optical methods, multimodal diagnostic techniques enable comprehensive disease characterization and significantly improve diagnostic accuracy by multidimensional characterization of tissue properties, physiological functions, and pathological changes.[25,124] These modalities function synergistically: optical imaging offers structural data at cellular resolution, and MRI excels in providing soft-tissue contrast and delineating anatomical structures. At the same time, PET quantifies metabolic activity to enable early lesion detection.[124] Importantly, deep-penetrating techniques such as CT, MRI, PET, and PAI[123–126] complement FLI, thereby effectively overcoming the inherent penetration-depth limitations of fluorescence signals.

Cyanine dyes possess a distinctive dual functionality: they are not only effective for FLI, but can also be engineered into excellent photothermal converters for PAI.[127,128] The photothermal conversion efficiency is primarily determined by the absorption coefficient and photothermal conversion ability of dyes, without the need for molecular redesign.[25] Utilizing this mechanism, Zhou *et al.*[124] constructed an orthogonal charge-transfer dyad, tricyanofuran (TCF)-containing heptamethine cyanine (TCF-Cy7(Py)-TCF), by introducing a cationic pyridine group at the *meso*-position of an anionic heptamethine cyanine dye (TCF-Cy7-TCF) (Fig. 11A). The TCF and the pyridine conferred excellent crystallization properties on TCF-CY(Py)-TCF and enhanced its photothermal conversion efficiency

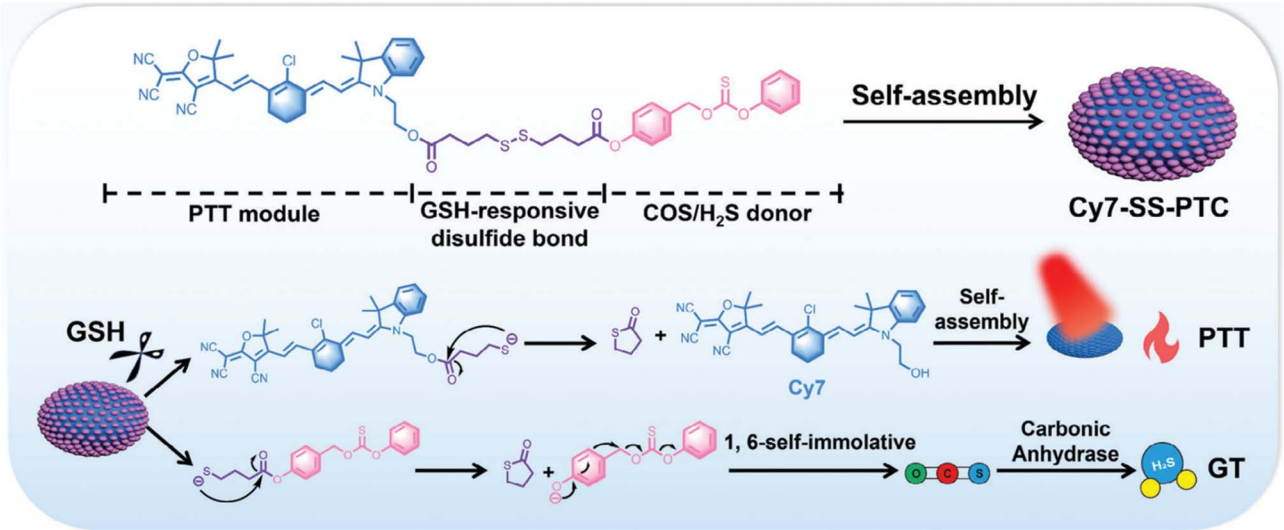

Fig. 12 Molecular structure and H_2S release mechanism of Cy7-SS-PTC NPs, and the schematic illustration of H_2S-assisted synergistic tumor photothermal therapy. Reprinted with permission from ref. 135, copyright 2025 Wiley.

from 7.78% to 55.06%, which was beneficial for exhibiting excellent PAI signals. This engineered nanoplatform achieved a high signal-to-noise ratio for tumor PAI/FLI imaging within the NIR window and demonstrated significant phototherapy efficacy after target accumulation (Fig. 11B–E).

3.3.2. Synergistic treatment. The inherent complexity of cancer, characterized by pathological diversity, metastasis, and high recurrence rates, renders single-modality treatment insufficient in clinical practice. Despite benefits such as NIR excitation, low phototoxicity, and multiple antitumor mechanisms, cyanine-dye-based phototherapy remains constrained by tumor heterogeneity and metastatic potential. Therefore, integrating phototherapy with other treatment modalities such as chemotherapy,[49,130] radiotherapy,[131–133] gas therapy,[134,135] and immunotherapy[32,63] represents a promising strategy to enhance therapeutic efficacy through complementary mechanisms.

(a) Chemo-phototherapy. Chemotherapy remains the cornerstone of clinical tumor management. The engineered integration of chemotherapy and phototherapy has emerged as a promising strategy to address the challenges posed by malignant tumors.[136] Cyanine dye-based chemo-phototherapy nanoplatforms offer distinct advantages, including spatiotemporally controlled drug release, reduced systemic dosage, mitigated drug resistance, and synergistic therapeutic effects.

In addition to traditional covalent drug–dye conjugates[130,137–140] and co-encapsulation systems,[49,141] emerging dye–drug co-assembly strategy[48,142,143] represents an advanced design paradigm for such synergistic agents. The cyanine dye–drug co-assembly employs supramolecular recognition mechanisms, such as hydrogen bonding, π–π stacking, and electrostatic interactions, to drive the spontaneous formation of nanodrugs. This approach not only enhances therapeutic payload concentration but also optimizes key pharmaceutical properties through synergic effects, ultimately improving drug stability, solubility, and bioavailability. Crucially, the spatiotemporally synchronized release of diagnostic and therapeutic agents from these nanotheranostics enables precise tumor targeting and synergic treatment.

(b) Synergetic photo/gas therapy. Tumor heterogeneity may lead to uneven distribution of dyes within tumors, combined with reduced light transmission capacity and heat loss caused by blood perfusion. These factors collectively weaken the efficacy of phototherapy, resulting in incomplete tumor clearance, ultimately contributing to recurrence and metastasis. Gaseous molecules such as nitric oxide (NO), carbon monoxide (CO), and hydrogen sulfide (H_2S) diffuse rapidly within tumors and possess intrinsic physiological functions,[135] effectively complementing the limitations of photosensitizers. For instance, CO and H_2S can reduce inflammation through the mitogen-activated protein kinase (MAPK) pathway. In contrast, NO reacts with superoxide anion radicals ($\cdot O_2^-$) to form peroxynitrite ($ONOO^-$), which can activate matrix metalloproteinases (MMPs) to degrade collagen and disrupt the extracellular matrix (ECM) barrier, thereby enhancing intratumoral accumulation. Notably, H_2S exhibits a concentration-dependent effect in tumors: low concentrations promote tumorigenesis by inducing angiogenesis, inhibiting apoptosis, enhancing mitochondrial metabolism, and accelerating the cell cycle; in contrast, high concentrations exert cytotoxic effects through mitochondrial respiration inhibition, adenosine triphosphate (ATP) synthesis disruption, and heat shock protein (HSP) expression downregulation.

Gas-phototheranostic agents are typically developed by either integrating gas-donor moieties into the structure of cyanine dyes[134,135,144] or by co-assembling such moieties with dye molecules.[145,146] Zhou *et al.*[135] conjugated the photosensitizer Cy7 with the H_2S donor phenylthiocarbonate (PTC) through a disulfide linkage, fabricating carrier-free nanoparticles (Cy7-SS-PTC; Fig. 12). Within the tumor microenvironment, overexpressed GSH triggered a cleavage of the disulfide bond, thus

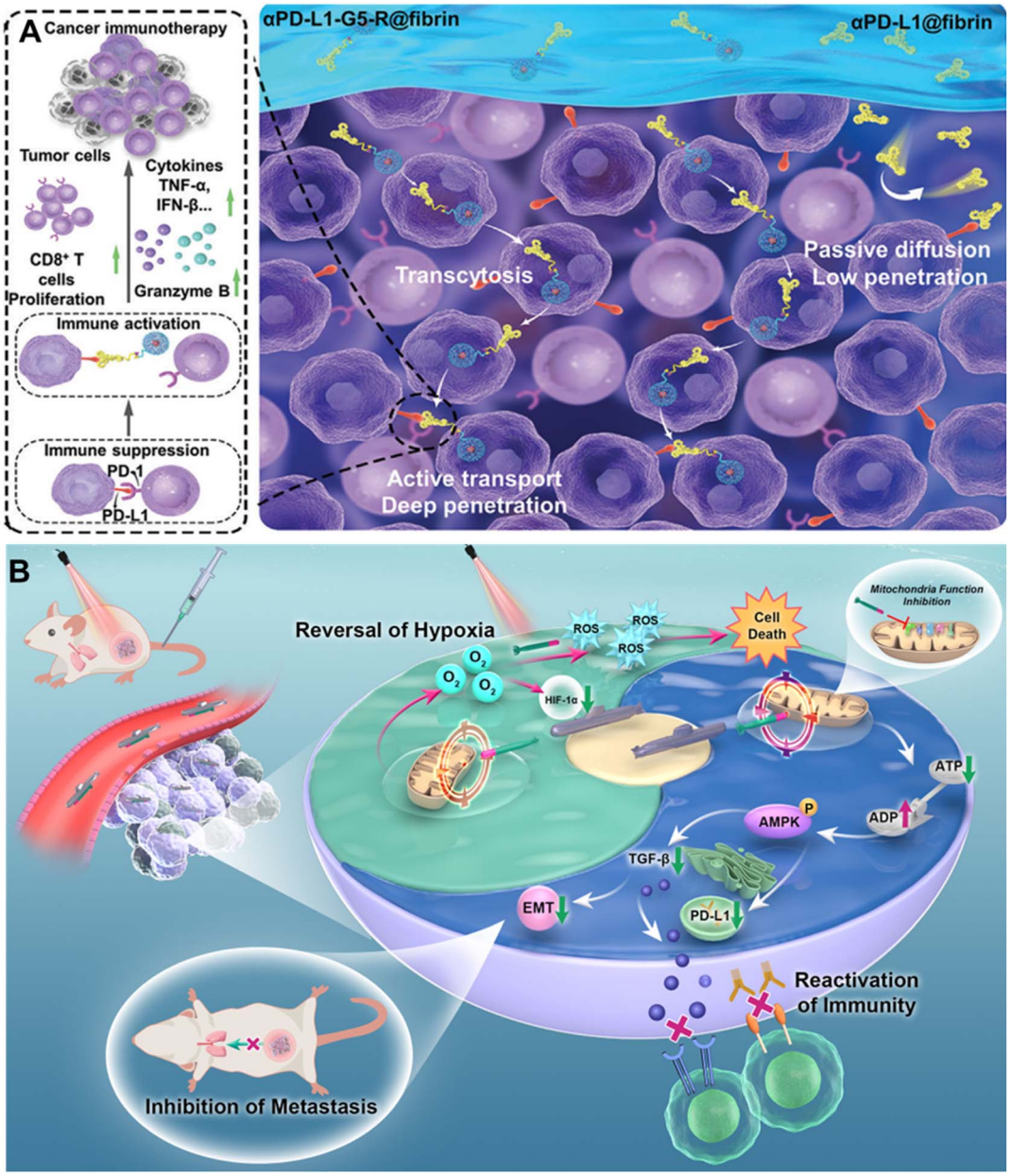

Fig. 13 (A) Illustration of Cy5 nanodots αPD-L1 conjugates (Cy5 nanodots-αPD-L1 conjugates) loaded in fibrin gels (αPD-L1-G5-R@fibrin). Reprinted with permission from ref. 150, copyright 2023 Wiley. (B) Preparation process of MHI-TMX@ALB nanoparticles and the mechanisms for enhancing photoimmunotherapy *via* highly efficient TGF-β and PD-L1 dual-depression. Reprinted with permission from ref. 151, copyright 2024 American Chemical Society.

initiating a cascade release of both Cy7 and H_2S. Under 808 nm laser irradiation, Cy7 simultaneously generates fluorescence and photoacoustic signals while generating photothermal effects, enabling integrated tumor theranostics. Concurrently, the released H_2S disrupts mitochondrial respiration, inhibits ATP synthesis, and downregulates HSP70 expression, thereby synergistically enhancing the photothermal efficacy and achieving an 88% tumor suppression rate.

(c) Photoimmunotherapy. The essence of phototherapy in activating antitumor immune responses is inducing immunogenic cell death.[147–149] However, immunosuppressive solid tumors formed an "immune brake" mechanism through the overexpression of checkpoint molecules (such as PD-L1 and cytotoxic T lymphocyte-associated antigen-4), infiltration of regulatory T cells, and secretion of immunosuppressive cytokines (such as transforming growth factor-β (TGF-β) and interleukin-10). This will ultimately weaken the immune response triggered by phototherapy. Therefore, integrating immune checkpoint inhibitors (ICIs) has become one of the most important strategies to reverse immune suppression. By selectively blocking T cell inhibitory signals, ICIs can amplify the immune activation induced by phototherapy, transforming local ablation into systemic immune surveillance. Zhou *et al.*[150] constructed a nanostructure by conjugating Cy5-labeled

polylysine dendrimers with surface-anchored anti-PD-L1 (αPD-L1) through a copper-free click reaction (Fig. 13A). The nanostructure facilitated global αPD-L1 delivery into tumors through adsorption-mediated endocytosis, which enhanced checkpoint blockade efficacy, reduced tumor recurrence rates, and significantly prolonged mouse survival.

In addition, Zhang *et al.*[32] conjugated a cyanine photosensitizer with a PD-1 inhibitor to actively recognize and block PD-1/PD-L1 binding between T cells and tumor cells. By this strategy, they effectively reversed the immunosuppressive microenvironment and prevented tumor cell immune evasion. In the hypoxic tumor microenvironment, cyanine dyes were activated, which then induced tumor cell pyroptosis *via* highly efficient PDT and further remodeled the immune microenvironment. This dual-action strategy, combining light-induced pyroptosis and PD-1 blockade, initiated a sequential cascade reaction of "immune activation – tumor microenvironment reprogramming – escape prevention", thereby achieving potent tumor immunotherapy.

Beyond exogenous checkpoint inhibitors, downregulating tumor PD-L1 expression through metabolic reprogramming represents a promising approach for converting tumors from low immunogenicity to high immunogenicity.[48,133,151] Shen[151] developed an albumin-based nanocarrier loaded with the cyanine dye MHI-148 that conjugated with tamoxifen, a clinically approved mitochondrial metabolism modulator (Fig. 13B). This nanoplatform simultaneously reversed tumor hypoxia and suppressed PD-L1/TGF-β expression through tamoxifen-mediated metabolic reprogramming, thereby enhancing T-cell infiltration and inhibiting 4T1 tumor lung metastasis. This synergistic epigenetic and metabolic reprogramming alleviates dual immunosuppression, enabling highly efficient fluorescence-guided PDT.

3.4. Optimizing photodynamic mechanisms

PDT serves as a core anti-tumor mechanism of cyanine dyes. Its fundamental principle lies in the synergistic effect of photosensitizers, light, and tissue oxygen to generates ROS.[152] Excessive ROS can further induce apoptosis or necrosis in tumor cells while causing negligible damage to surrounding normal tissues. To date, numerous studies have systematically elucidated the core mechanisms of PDT.[153,154] Among these, Kozlikova *et al.*[155] noted that the photodynamic activity of dyes is closely related to their ability to generate singlet oxygen and their aggregation state. Furthermore, the type of PDT directly determines its tumor-killing potency and its adaptability to the hypoxic tumor microenvironment.

The type of PDT is primarily determined by the mechanism of ROS generation and can be classified into Type I and Type II. Type II PDT involves energy transfer from the photosensitizer to oxygen, producing $^1O_2$. Type I PDT generates ROS (such as $\cdot O_2^-$, hydroxyl radicals (·OH), and hydrogen peroxide) through electron transfer with surrounding water and oxygen. Crucially, heteropolar reactions and the Haber-Weiss/Fenton cycle enable efficient generation of $\cdot O_2^-$ and ·OH even under severe hypoxic conditions, with significantly lower oxygen dependence at the target site.[86,156] Therefore, Type I PDT demonstrates superior efficacy against hypoxic solid tumors. In type I PDT, ROS generation relies on electron transfer, in which the formation of a charge-separated state (CSS) within the PS is a critical step. A common strategy for achieving efficient charge separation involves constructing an electron donor–acceptor molecular system.[157,158] Prolonging the lifetime of the CSS is crucial to provide sufficient time for electron transfer, which drives research into molecular structural modulation. By inserting bridging groups between the donor and acceptor moieties, charge recombination can be effectively suppressed, thereby stabilizing the CSS. Additionally, transformation from local to non-local CSS through symmetry-breaking charge separation during molecular self-assembly can generate reactive anionic and cationic free radicals. Based on this principle, Fan *et al.*[159,160] designed a series of *meso*-modified, heavy-atom-free NIR photosensitizers that could self-assemble into nanoparticles in aqueous media. Through light-induced cascade charge transfer processes, these photosensitizers generated substantial ·OH for highly efficient phototherapy of hypoxic tumors.

Compared to the rapid energy transfer characteristic of Type II PDT, the electron transfer process in Type I PDT is relatively slower. Extending the triplet excited state (T_1) lifetime of photosensitizers thus represents another key strategy for improving electron transfer efficiency. This can be achieved through dye structural design and by adjusting the spatial arrangement of intramolecular electron donors and acceptors.[161] Guided by this approach, Guo[86] introduced a naphthyl imide group as an electron acceptor at the *meso* position of a Cy5 electron donor scaffold. In the resulting molecular structure, the acceptor and the Cy5 donor adopt a nearly perfect orthogonal geometry with high structural rigidity. Upon forming an intracellular sandwich-like π–π stacking assembly between the *N*-benzyl and naphthalimide units, this system not only extended T_1 lifetime (up to 389 μs), but also significantly boosts $\cdot O_2^-$ generation. Remarkably, after a single *in vivo* PDT treatment, the tumor was almost completely eradicated.

4. Conclusions and outlooks

As readily engineerable NIR fluorophores, cyanine dyes hold significant promise for integrated cancer theranostics. This review systematically outlines strategies for cyanine dye modulation, encompassing both direct molecular modifications and nanostructure construction, to achieve precise tumor targeting, high-fidelity imaging, and efficient tumor ablation. As a light-activated theranostic platform, cyanine dyes pose challenges, including photochemical instability, limited excitation wavelength, and suboptimal treatment efficiency. Strategic molecular and supramolecular engineering, particularly structural modification and aggregate regulation, can red-shift excitation profiles. This spectral extension substantially enhances photostability while elevating diagnostic sensitivity and therapeutic potency.

In terms of diagnosis, the integration of optical diagnosis with complementary imaging modalities (*e.g.*, CT, MRI) enables

the development of synergistic systems. These systems combine high spatiotemporal resolution, molecular sensitivity, and deep-tissue penetration to overcome the inherent limitations of standalone optical techniques. In therapeutic applications, multimodal combination therapy, which integrates phototherapy with chemotherapy, gas therapy, and immunotherapy, can effectively address monotherapy's critical obstacles, including oxygen dependency, tumor recurrence, and metastasis. Although cyanine dye-based phototheranostics have been well developed for tumor treatment, several challenges remain in advancing their practical use.

(1) Pharmacokinetic and biodistribution challenges. Despite demonstrating excellent spatiotemporal controllability, biosafety, and tumor-targeting capabilities *in vivo* through structural optimization, cyanine dye-based theranostics still face significant obstacles in dynamic distribution. Real-time dynamic biodistribution mapping remains technically challenging, hindering the precise correlation between agent localization and therapeutic efficacy. Additionally, tumor heterogeneity frequently leads to uneven intratumoral distribution, generating treatment blind spots that cannot be detected by current imaging modalities. To overcome these limitations, it is necessary to integrate multimodal analytical techniques. By combining real-time imaging with mass spectrometry and computational modeling, *in vivo* distribution and metabolic behavior, key requirements for clinical translation, can be comprehensively simulated and analyzed.

(2) AI-enabled molecular design. The rapid evolution of artificial intelligence, particularly machine learning algorithms, offers transformative potential for accelerating development cycles. Computational approaches can predictively optimize cyanine dye structures and self-assembly configurations, enabling rational design of next-generation agents. This paradigm shift will revolutionize both synthesis protocols and performance evaluation, allowing high-throughput virtual screening of photophysical properties, tumor-targeting efficiency, and metabolic stability before experimental validation.

(3) Synthesis scalability barriers. Current synthetic routes for structurally sophisticated cyanine dyes involve labour-intensive, multi-step processes with suboptimal reaction yields. These complexities, particularly for dyes requiring precise stereochemistry or polycyclic architectures, severely constrain large-scale production. Streamlining synthetic protocols through catalytic innovation, continuous-flow chemistry, and an automated purification system is needed to improve reaction efficiency and yield. Such process intensification will facilitate clinical-grade manufacturing while reducing production costs.

Conflicts of interest

There are no conflicts to declare.

Data availability

No primary research results, software, or code have been included, and no new data were generated or analysed as part of this review.

Acknowledgements

The authors thank financial support from the National Natural Science Foundation of China (grant no. 52325304, 32301201), and the Northwest A & F University Startup Fund.

References

1 B. Wang, S. Hu, Y. Teng, J. Chen, H. Wang, Y. Xu, K. Wang, J. Xu, Y. Cheng and X. Gao, Current advance of nanotechnology in diagnosis and treatment for malignant tumors, *Signal Transduction and Targeted Ther.*, 2024, **9**, 200.
2 D. F. Quail and J. A. Joyce, Microenvironmental regulation of tumor progression and metastasis, *Nat. Med.*, 2013, **19**, 1423–1437.
3 A. F. Chambers, G. N. Naumov, H. J. Varghese, K. V. Nadkarni, I. C. MacDonald and A. C. Groom, Critical steps in hematogenous metastasis: an overview, *Surg. Oncol. Clin. North Am.*, 2001, **10**, 243–255.
4 E. R. Pereira, D. Kedrin, G. Seano, O. Gautier, E. F. J. Meijer, D. Jones, S.-M. Chin, S. Kitahara, E. M. Bouta, J. Chang, E. Beech, H.-S. Jeong, M. C. Carroll, A. G. Taghian and T. P. Padera, Lymph node metastases can invade local blood vessels, exit the node, and colonize distant organs in mice, *Science*, 2018, **359**, 1403–1407.
5 WHO, Global cancer burden growing, amidst mounting need for services, *Saudi Med. J.*, 2024, **3**, 326–327.
6 S. Zeng, Z. Guo, Y. Hao, Y. S. Kafuti, Z. Yang, Q. Yao, J. Wang, X. Peng and H. Li, Tumor-microenvironment-activatable organic phototheranostic agents for cancer therapy, *Coord. Chem. Rev.*, 2024, **509**, 215786.
7 Z. Pei, H. Lei and L. Cheng, Bioactive inorganic nanomaterials for cancer theranostics, *Chem. Soc. Rev.*, 2023, **52**, 2031–2081.
8 A. Sharma, P. Verwilst, M. Li, D. Ma, N. Singh, J. Yoo, Y. Kim, Y. Yang, J.-H. Zhu, H. Huang, X.-L. Hu, X.-P. He, L. Zeng, T. D. James, X. Peng, J. L. Sessler and J. S. Kim, Theranostic fluorescent probes, *Chem. Rev.*, 2024, **124**, 2699–2804.
9 E. A. Perez, E. H. Romond, V. J. Suman, J.-H. Jeong, G. Sledge, C. E. Geyer, S. Martino, P. Rastogi, J. Gralow, S. M. Swain, E. P. Winer, G. Colon-Otero, N. E. Davidson, E. Mamounas, J. A. Zujewski and N. Wolmark, Trastuzumab plus adjuvant chemotherapy for human epidermal growth factor receptor 2-positive breast cancer: planned joint analysis of overall survival from NSABP B-31 and NCCTG N9831, *J. Clin. Oncol.*, 2014, **32**, 3744–3752.
10 P. Choudhury and M. Gupta, Personalized & precision medicine in cancer: a theranostic approach, *Curr. Radiopharm.*, 2017, **10**, 166–170.
11 Y.-F. Ou, H.-Y. Xiang, X. Yang, R.-X. Wang, S.-Y. Huan, L. Yuan, T.-B. Ren and X.-B. Zhang, Constructing stable and wavelength-extended heptamethine cyanines via donor ectopic substitution for NIR-IIa/b Bioimaging, *Angew. Chem., Int. Ed.*, 2025, **64**, e202423978.
12 J. Lu, J. Ding, Z. Xia, Z. Yang, C. Lv, S. Zong, J. Cao, D. Zhou, S. Long, W. Sun, J. Du, J. Fan and X. Peng, Spin

Manipulation Engineering of Photodynamic Intermediates: Magnetic Amplification of Oxyradicals Generation for Enhanced Antitumor Phototherapeutic Efficacy, *J. Am. Chem. Soc.*, 2025, **147**, 18100–18109.

13 A. Józefczak, K. Kaczmarek and R. Bielas, Magnetic mediators for ultrasound theranostics, *Theranostics*, 2021, **11**, 10091–10113.

14 H. J. Krause and U. M. Engelmann, Fundamentals and Applications of Dual-Frequency Magnetic Particle Spectroscopy: Review for Biomedicine and Materials Characterization, *Adv. Sci.*, 2025, **12**, 2416838.

15 Y. Zhang, X. Wang, C. Chu, Z. Zhou, B. Chen, X. Pang, G. Lin, H. Lin, Y. Guo, E. Ren, P. Lv, Y. Shi, Q. Zheng, X. Yan, X. Chen and G. Liu, Genetically engineered magnetic nanocages for cancer magneto-catalytic theranostics, *Nat. Commun.*, 2020, **11**, 5421.

16 M. Yin, Y. Yuan, Y. Huang, X. Liu, F. Meng, L. Luo, S. Tian and B. Liu, Carbon–Iodine Polydiacetylene Nanofibers for Image-Guided Radiotherapy and Tumor-Microenvironment-Enhanced Radiosensitization, *ACS Nano*, 2024, **18**, 8325–8336.

17 J. Wang, J. W. Seo, A. J. Kare, M. Schneider, M. Pandrala, S. K. Tumbale, M. N. Raie, G. Engudar, N. Zhang, Y. Guo, X. Zhong, S. Ferreira, B. Wu, L. D. Attardi, G. Pratx, A. Iagaru, R. L. Brunsing, G. W. Charville, W. G. Park and K. W. Ferrara, Spatial transcriptomic analysis drives PET imaging of tight junction protein expression in pancreatic cancer theranostics, *Nat. Commun.*, 2024, **15**, 10751.

18 A. T. Tran, E. O. Wisniewski, P. Mistriotis, K. Stoletov, M. Parlani, A. Amitrano, B. Ifemembi, S. J. Lee, K. Bera, Y. Zhang, S. Tuntithavornwat, A. Afthinos, A. Kiepas, B. Agarwal, S. Nath, J. J. Jamieson, Y. Zuo, D. Habib, P.-H. Wu, S. S. Martin, S. Gerecht, L. Gu, J. D. Lewis, P. Kalab, P. Friedl and K. Konstantopoulos, Cytoplasmic anillin and Ect2 promote RhoA/myosin II-dependent confined migration and invasion, *Nat. Mater.*, 2025, **24**, 1476–1488.

19 D. T. Nguyen, M. J. Baek, S. M. Lee, D. Kim, S. Y. Yoo, J. Y. Lee and D. D. Kim, Photobleaching-mediated charge-convertible cyclodextrin nanoparticles achieve deep tumour penetration for rectal cancer theranostics, *Nat. Nanotechnol.*, 2024, **19**, 1723–1734.

20 S. Jiang, W. Li, B. Li, S. Chen, S. Lei, Y. Liu, J. Lin and P. Huang, Albumin-Energized NIR-II Cyanine Dye for Fluorescence/Photoacoustic/Photothermal Multi-Modality Imaging-Guided Tumor Homologous Targeting Photothermal Therapy, *J. Med. Chem.*, 2025, **68**, 3324–3334.

21 X. Wang, B. Cui, Q. Sun, H. Liu and Z. Liu, Small-molecule photoacoustic probes for *in vivo* imaging, *Chem. Soc. Rev.*, 2025, **54**, 8809–8844.

22 D. Zhao, L. Zhang, M. Yin, Z. He, F. Fang, M. Zhan, S. Tian, F. Meng and L. Luo, Atomic-iodine-substituted polydiacetylene nanospheres with boosted intersystem crossing and nonradiative transition through complete radiative transition blockade for ultraeffective phototherapy, *Aggregate*, 2024, **5**, e576.

23 J. Yuan, H. Yang, W. Huang, S. Liu, H. Zhang, X. Zhang and X. Peng, Design strategies and applications of cyanine dyes in phototherapy, *Chem. Soc. Rev.*, 2025, **54**, 341–366.

24 Y. Zhang, B. Wang, Q. Yan, X. Lu, X. Zhang, C. Yao, Y. Qi, M. Yang, G. Ge, X. Qian, X. Luo and Y. Yang, Super-Absorbing Quantum-Confined Cyanine Dyes for NearInfrared Confocal Imaging of Hierarchical Nephron Structures, *J. Am. Chem. Soc.*, 2025, **147**, 40739–40750.

25 W. Liu, C. Lv, Y. Hou, X. Lou, Z. Ma, M. He, X. Zeng, W. Sun, J. Fan and X. Peng, A cyanine fluorophore for imaging-guided tumor photodynamic and photothermal therapy under NIR-II light activation, *Sci. China Chem.*, 2025, **68**, 5065–5073.

26 A. A. Ishchenko, The length of the polymethine chain and the spectral-luminescent properties of symmetrical cyanine dyes, *Russ. Chem. Bull.*, 1994, **43**, 1161–1174.

27 H. Fukushima, S. S. Matikonda, S. M. Usama, A. Furusawa, T. Kato, L. Štacková, P. Klán, H. Kobayashi and M. J. Schnermann, Cyanine Phototruncation Enables Spatiotemporal Cell Labeling, *J. Am. Chem. Soc.*, 2022, **144**, 11075–11080.

28 L. Štacková, E. Muchová, M. Russo, P. Slavíček, P. Štacko and P. Klán, Deciphering the Structure-Property Relations in Substituted Heptamethine Cyanines, *J. Org. Chem.*, 2020, **85**, 9776–9790.

29 S. M. Usama, S. C. Marker, D.-H. Li, D. R. Caldwell, M. Stroet, N. L. Patel, A. G. Tebo, S. Hernot, J. D. Kalen and M. Schnermann, Method To Diversify Cyanine Chromophore Functionality Enables Improved Biomolecule Tracking and Intracellular Imaging, *J. Am. Chem. Soc.*, 2023, **145**, 14647–14659.

30 A. V. Kulinich and A. A. Ishchenko, Design and Photonics of Merocyanine Dyes, *Chem. Rec.*, 2024, **24**, e202300262.

31 X. Zhao, Q. Yao, S. Long, W. Chi, Y. Yang, D. Tan, X. Liu, H. Huang, W. Sun, J. Du, J. Fan and X. Peng, An Approach to Developing Cyanines with Simultaneous Intersystem Crossing Enhancement and Excited-State Lifetime Elongation for Photodynamic Antitumor Metastasis, *J. Am. Chem. Soc.*, 2021, **143**, 12345–12354.

32 P. Z. Liang, L. L. Ren, Y. H. Yan, Z. Li, F. Y. Yang, T. B. Ren, L. Yuan and X. B. Zhang, Activatable Photosensitizer Prodrug for Self-Amplified Immune Therapy Via Pyroptosis, *Angew. Chem., Int. Ed.*, 2025, **64**, e202419376.

33 Y. Qiu, B. Yuan, Y. Cao, X. He, O. U. Akakuru, L. Lu, N. Chen, M. Xu, A. Wu and J. Li, Recent progress on near-infrared fluorescence heptamethine cyanine dye-based molecules and nanoparticles for tumor imaging and treatment, *Wiley Interdiscip. Rev.:Nanomed. Nanobiotechnol.*, 2023, **15**, e1910.

34 L. Štacková, M. Russo, L. Muchová, V. Orel, L. Vítek, P. Štacko and P. Klán, Cyanine-Flavonol Hybrids for Near-Infrared Light-Activated Delivery of Carbon Monoxide, *Chem. – Eur. J.*, 2020, **26**, 13184–13190.

35 N. Bel'ko, A. Mal'tanova, A. Bahdanava, A. Lugovski, S. Fatykhava, P. Shabunya, A. Smaliakou, S. Poznyak, T. Kulahavac and M. Samtsov, A near-infrared superoxide generator based on a biocompatible indene-bearing

heptamethine cyanine dye, *J. Mater. Chem. B*, 2024, **12**, 11202–11209.
36 A. A. Lugovski, M. P. Samtsov, K. N. Kaplevsky, D. Tarasau, E. S. Voropay, P. T. Petrov and Y. P. Istomin, Novel indotricarbocyanine dyes covalently bonded to polyethylene glycol for theranostics, *J. Photochem. Photobiol., A*, 2016, **316**, 31–36.
37 H. Janeková, M. Russo and P. Štacko, Cyanine Renaissance: Tailoring the Properties to Applications, *Chimia*, 2022, **76**, 763–771.
38 X. Ma, Y. Huang, A. Li, X. Zeng, S. H. Liu, J. Yin and G.-F. Yang, The Aggregates of Near-Infrared Cyanine Dyes in Phototherapy, *ChemMedChem*, 2023, **18**, e202300204.
39 Y. Gao, L. Zhu, Z. Du, J. Xiong, R. Ma, M. Aili, N. Alifu and B. Dong, Recent Advances in Near-Infrared Cyanine Dye-Based Fluorescent Nanoprobes for Tumor Imaging and Therapy, *Int. J. Nanomed.*, 2025, **20**, 13911–13937.
40 J. Zhang, W. Wang, J. Shao, J. Chen and X. Dong, Small molecular cyanine dyes for phototheranostics, *Coord. Chem. Rev.*, 2024, **516**, 215986.
41 P. Bhattarai and Z. Dai, Cyanine based Nanoprobes for Cancer Theranostics, *Adv. Healthcare Mater.*, 2017, **6**, 1700262.
42 P. J. Choi, T. I. Park, E. Cooper, M. Dragunow, W. A. Denny and J. Jose, Heptamethine Cyanine Dye Mediated Drug Delivery: Hype or Hope, *Bioconjugate Chem.*, 2020, **31**, 1724–1739.
43 L. Zhang, H. Jia, X. Liu, Y. Zou, J. Sun, M. Liu, S. Jia, N. Liu, Y. Li and Q. Wang, Heptamethine Cyanine-Based Application for Cancer Theranostics, *Front. Pharmacol.*, 2021, **12**, 764654.
44 Z. Kejík, J. Hajduch, N. Abramenko, F. Vellieux, K. Veselá, J. Leischner Fialová, K. Petrláková, K. Kučnirová, R. Kaplánek, A. Tatar, M. Skaličková, M. Masařík, P. Babula, P. Dytrych, D. Hoskovec, P. Martásek and M. Jakubek, Cyanine dyes in the mitochondria targeting photodynamic and photothermal Therapy, *Commun. Chem.*, 2024, **7**, 180.
45 Y. Gao, L. Zhu, Z. Du, J. Xiong, R. Ma, M. Aili, N. Alifu and B. Dong, Recent Advances in Near-Infrared Cyanine Dye-Based Fluorescent Nanoprobes for Tumor Imaging and Therapy, *Int. J. Nanomed.*, 2025, **20**, 13911–13937.
46 L. Wang, J. Li, Z. Zhao, Y. Xia, Y. Xie, D. Hong, Y. Liu and W. Tan, Aptamer Conjugate-Based Ratiometric Fluorescent Probe for Precise Imaging of Therapy-Induced Cancer Senescence, *Anal. Chem.*, 2024, **96**, 154–162.
47 M. Shi, Y. Li, W. Pan, Z. Fu, K. Wang, X. Liu, N. Li and B. Tang, A BRD4-Targeting Photothermal Agent for Controlled Protein Degradation, *Angew. Chem., Int. Ed.*, 2024, **63**, e202403258.
48 J. Liu, M. Wu, Q. Lyu, C. Yang, N. Fan, K. Chen and W. Wang, IR783-Stabilized Nanodrugs Enhance Anticancer Immune Response by Synergizing Oxidation Therapy and Epigenetic Modulation, *Adv. Sci.*, 2025, **12**, 2415684.
49 Z. Wang, S. Zhang, Z. Kong, S. Li, J. Sun, Y. Zheng, Z. He, H. Ye and C. Luo, Self-adaptive nanoassembly enabling turn-on hypoxia illumination and periphery/center closed-loop tumor eradication, *Cell Rep. Med.*, 2023, **4**, 101014.
50 B. Li, J. Tian, F. Zhang, C. Wu, Z. Li, D. Wang, J. Zhuang, S. Chen, W. Song, Y. Tang, Y. Ping and B. Liu, Self-assembled aldehyde dehydrogenase-activatable nano-prodrug for cancer stem cell-enriched tumor detection and treatment, *Nat. Commun.*, 2024, **15**, 9417.
51 L. Xu, N. Liu, W. Zhan, Y. Deng, Z. Chen, X. Liu, G. Gao, Q. Chen, Z. Liu and G. Liang, Granzyme B Turns Nanoparticle Fluorescence "On" for Imaging Cytotoxic T Lymphocyte Activity in Vivo, *ACS Nano*, 2022, **16**, 19328–19334.
52 P. Lin, Y. Xue, X. Mu, Y. Shao, Q. Lu, X. Jin, E. Yinwang, Z. Zhang, H. Zhou, W. Teng, H. Sun, W. Chen, W. Shi, C. Shi, X. Zhou, X. Jiang, X. Yu and Z. Ye, Tumor Customized 2D Supramolecular Nanodiscs for Ultralong Tumor Retention and Precise Photothermal Therapy of Highly Heterogeneous Cancers, *Small*, 2022, **18**, 2200179.
53 F. Würthner, T. E. Kaiser and C. R. Saha-Möller, J-Aggregates: From Serendipitous Discovery to Supramolecular Engineering of Functional Dye Materials, *Angew. Chem., Int. Ed.*, 2011, **50**, 3376–3410.
54 S. Xu, H. W. Liu, S. Y. Huan, L. Yuan and X. B. Zhang, Recent progress in utilizing near-infrared J-aggregates for imaging and cancer therapy, *Mater. Chem. Front.*, 2021, **5**, 1076–1089.
55 M. Kasha, Energy transfer mechanisms and the molecular exciton model for molecular aggregates, *Radiat. Res.*, 1963, **20**, 55–70.
56 K. Jasper, Modeling the optical properties of excitons in linear and tubular J-aggregates, *Int. J. Photoenergy*, 2006, **2006**, 61364.
57 H. Piwoński, S. Nozue, H. Fujita, T. Michinobu and S. Habuchi, Organic J-Aggregate Nanodots with Enhanced Light Absorption and Near-Unity Fluorescence Quantum Yield, *Nano Lett.*, 2021, **21**, 2840–2847.
58 E. E. Jelley, Spectral Absorption and Fluorescence of Dyes in the Molecular State, *Nature*, 1936, **138**, 1009–1010.
59 F. Y. Yang, Y. F. Ou, J. L. Zhou, P. Z. Liang, T. B. Ren, X. B. Zhang and L. Yuan, Hydrogen-Bond Network-Directed Controllable Assembly of Stable Cyanine J-Aggregates for Long-Term and High-Contrast In Vivo Imaging, *Angew. Chem., Int. Ed.*, 2026, **138**, e24960.
60 M. Li, W. Sun, R. Tian, J. Cao, Y. Tian, B. Gurram, J. Fan and X. Peng, Smart J-aggregate of cyanine photosensitizer with the ability to target tumor and enhance photodynamic therapy efficacy, *Biomaterials*, 2021, **269**, 120532.
61 S. M. Usama, G. K. Park, S. Nomura, Y. Baek, H. S. Choi and K. Burgess, Role of Albumin in Accumulation and Persistence of Tumor-Seeking Cyanine Dyes, *Bioconjugate Chem.*, 2020, **31**, 248–259.
62 L. Bai, Y. Jia, Z. Wang, Z. Wang, Y. Jia, Y. Zhang and S. Zhu, Albumin Encapsulation of Cyanine Dye for High-Performance NIR-II Imaging-Guided Photodynamic Therapy, *Chem. Biomed. Imaging*, 2025, **3**, 424–432.
63 C. Gerke, I. Zabala Gutierrez, D. Mendez-Gonzalez, M. C. I. Cruz, F. Mulero, D. Jaque and J. Rubio-Retama,

Clickable Albumin Nanoparticles for Pretargeted Drug Delivery toward PD-L1 Overexpressing Tumors in Combination Immunotherapy, *Bioconjugate Chem.*, 2022, **33**, 821–828.

64 S. Luo, X. Luo, X. Wang, L. Li, H. Liu, B. Mo, H. Gan, W. Sun, L. Wang, H. Liang and S. Yu, Tailoring Multifunctional Small Molecular Photosensitizers to *In Vivo* Self-Assemble with Albumin to Boost Tumor-Preferential Accumulation, NIR Imaging, and Photodynamic/Photothermal/Immunotherapy, *Small*, 2022, **18**, 2201298.

65 H. Luo, Z. Wang, Q. Mo, J. Yang, F. Yang, Y. Tang, J. Liu and X. Li, Framework Nucleic Acid-Based Multifunctional Tumor Theranostic Nanosystem for miRNA Fluorescence Imaging and Chemo/Gene Therapy, *ACS Appl. Mater. Interfaces*, 2023, **15**, 33223–33238.

66 S. Wang, Z. Liu, Y. Tong, Y. Zhai, X. Zhao, X. Yue, Y. Qiao, Y. Liu, Y. Yin, R. Xi, W. Zhao and M. Meng, Improved cancer phototheranostic efficacy of hydrophobic IR780 via parenteral route by association with tetrahedral nanostructured DNA, *J. Controlled Release*, 2021, **330**, 483–492.

67 Z. Li, Y. Wang, J. Liu, P. Rawding, J. Bu, S. Hong and Q. Hu, Chemically and Biologically Engineered Bacteria-Based Delivery Systems for Emerging Diagnosis and Advanced Therapy, *Adv. Mater.*, 2021, **33**, 2102580.

68 Z. Gao, E. Zhang, H. Zhao, S. Xia, H. Bai, Y. Huang, F. Lv, L. Liu and S. Wang, Bacteria-Mediated Intracellular Click Reaction for Drug Enrichment and Selective Apoptosis of Drug-Resistant Tumor Cells, *ACS Appl. Mater. Interfaces*, 2022, **14**, 12106–12115.

69 W. Chen, C. He, N. Qiao, Z. Guo, S. Hu, Y. Song, H. Wang, Z. Zhang, B. Ke and X. Sun, Dual drugs decorated bacteria irradiate deep hypoxic tumor and arouse strong immune responses, *Biomaterials*, 2022, **286**, 121582.

70 Y. Liu, J. Zhang, X. Zhou, Y. Wang, S. Lei, G. Feng, D. Wang, P. Huang and J. Lin, Dissecting Exciton Dynamics in pH-Activatable Long-Wavelength Photosensitizers for Traceable Photodynamic Therapy, *Angew. Chem., Int. Ed.*, 2024, **63**, e202408064.

71 X. Li, N. L. Patel, J. Kalen and M. J. Schnermann, Benzyl Ammonium Carbamates Undergo Two-Step Linker Cleavage and Improve the Properties of Antibody Conjugates, *Angew. Chem., Int. Ed.*, 2025, **64**, e202417651.

72 K. Hanaya, K. Taguchi, Y. Wada and M. Kawano, One-Step Maleimide-Based Dual Functionalization of Protein N-Termini, *Angew. Chem., Int. Ed.*, 2025, **64**, e202417134.

73 E. Thankarajan, H. Tuchinsky, S. Aviel-Ronen, A. Bazylevich, G. Gellerman and L. Patsenker, Antibody guided activatable NIR photosensitizing system for fluorescently monitored photodynamic therapy with reduced side effects, *J. Controlled Release*, 2022, **343**, 506–517.

74 E. R. Thapaliya, S. M. Usama, N. L. Patel, Y. Feng, J. D. Kalen, B. St. Croix and M. J. Schnermann, Cyanine Masking: A Strategy to Test Functional Group Effects on Antibody Conjugate Targeting, *Bioconjugate Chem.*, 2022, **33**, 718–725.

75 Y. L. Lee, Y. T. Chou, B. K. Su, C. C. Wu, C. H. Wang, K. H. Chang, J. A. A. Ho and P. T. Chou, Comprehensive Thione-Derived Perylene Diimides and Their Bio-Conjugation for Simultaneous Imaging, Tracking, and Targeted Photodynamic Therapy, *J. Am. Chem. Soc.*, 2022, **144**, 17249–17260.

76 S. F. A. Rizvi, N. Abbas, H. Zhang and Q. Fang, Identification of a pH-Responsive Peptide–Paclitaxel Conjugate as a Novel Drug with Improved Therapeutic Potential, *J. Med. Chem.*, 2023, **66**, 8324–8337.

77 B. Yang, Y. Yang, Y. Chen, S. Wu, W. Zhang, M. Zhu, S. Li, X. Jia, L. Gai and L. Feng, Mannose functionalized small molecule nanodrug self-assembled from amphiphilic prodrug connected by disulfide bonds for synergistic cancer chemotherapy and photodynamic/photothermal therapy, *Int. J. Pharm.*, 2025, **671**, 125238.

78 V. N. Nguyen, T. G. Nguyen Cao, H. Jeong, Q. Truong Hoang, B. T. T. Pham, J. Bang, C. W. Koh, J. H. Kang, J. H. Lee, X. Wu, W. J. Rhee, Y. T. Ko, K. M. K. Swamy, S. Park, J. Park, M. S. Shim and J. Yoon, Tumor-Targeted Exosome-Based Heavy Atom-Free Nanosensitizers With Long-Lived Excited States for Safe and Effective Sono-Photodynamic Therapy of Solid Tumors, *Adv. Healthcare Mater.*, 2025, **14**, 2500927.

79 J. Si, C. Li, X. Chen, Q. Zhou, Y. Xue, Y. Ji, Y. Dong and Z. Ge, A Near-Infrared Fluorescent Macromolecular Dye for Precise Identification of Glioblastoma Boundaries, *Bioconjugate Chem.*, 2025, **36**, 578–587.

80 P. Chen, Z. Lu, X. Feng, Y. Hu, Y. Qin, Y. Lu, F. Han and T. Li, Monomeric or Homodimer Conjugates of Fibroblast Activation Protein Inhibitor and Cyanine 7 Bearing a *Meso*-Chloride as Near-Infrared Fluorescence Probes: Design, Synthesis, and Comparative *In Vivo* Imaging of Distinct Breast Cancer Subtypes, *J. Med. Chem.*, 2025, **68**, 1417–1432.

81 R. Wang, Y. Yao, Y. Gao, M. Liu, Q. Yu, X. Song, X. Han, D. Niu and L. Jiang, CD133-Targeted Hybrid Nanovesicles for Fluorescent/Ultrasonic Imaging-Guided HIFU Pancreatic Cancer Therapy, *Int. J. Nanomed.*, 2023, **18**, 2539–2552.

82 A. Faust, N. Baumer, A. Schlutermann, M. Becht, L. Greune, C. Geyer, C. Ruter, R. Margeta, L. Wittmann, P. Dersch, G. Lenz, W. E. Berdel and S. Baumer, Tumor-Cell-Specific Targeting of Ibrutinib: Introducing Electrostatic Antibody-Inhibitor Conjugates (AiCs), *Angew. Chem., Int. Ed.*, 2022, **61**, e202109769.

83 Z. Gao, Z. Yang, Z. Li and K. Burgess, Fluorescent PARP Inhibitors Applied To Intracranial Glioblastoma: Accumulation and Persistence *In Vivo*, *ACS Med. Chem. Lett.*, 2022, **13**, 911–915.

84 X. Cai, W. Liu, J. Zhang, Z. Li, M. Liu, S. Hu, J. Luo, K. Peng, B. Ye, Y. Wang and R. Yan, Study of Iron Complex Photosensitizer with Hollow Double-Shell Nano Structure Used to Enhance Ferroptosis and Photodynamic Therapy, *Small*, 2024, **20**, 2309086.

85 Z. Hu, R. Li, X. Zhang and Z. Chen, A pH-responsive NIR fluorescent probe for precise cancer phototheranostics, *Sens. Actuators, B*, 2025, **440**, 137877.
86 G. Yao, J. Miao, Y. Huo and W. Guo, Improved Orthogonality in Naphthalimide/Cyanine Dyad Boosts Superoxide Generation: a Tumor-Targeted Type-I Photosensitizer for Photodynamic Therapy of Tumor by Inducing Ferroptosis, *Adv. Sci.*, 2025, **12**, 2417179.
87 A. Babu, S. Padmanaban, S. Chahal, A. Mohapatra, A. Sundaram, C. S. Cho and I. K. Park, Targeted nanoparticle delivery unleashes synergistic photothermal and immunotherapeutic effects against hepatocellular carcinoma, *J. Nanobiotechnol.*, 2024, **22**, 778.
88 Z. Pan, Y. Zeng, Z. Ye, Y. Li, Y. Wang, Z. Feng, Y. Bao, J. Yuan, G. Cao, J. Dong, W. Long, Y. J. Lu, K. Zhang, Y. He and X. Liu, Rotor-based image-guided therapy of glioblastoma, *J. Controlled Release*, 2024, **368**, 650–662.
89 Z. Hu, R. Li, X. Cui and Z. Chen, Albumin-Based Cyanine Crizotinib Conjugate Nanoparticles for NIR-II Imaging-Guided Synergistic Chemophototherapy, *ACS Appl. Mater. Interfaces*, 2023, **15**, 33890–33902.
90 D. Kobzev, O. Semenova, A. Tatarets, A. Bazylevich, G. Gellerman and L. Patsenker, Antibody-guided iodinated cyanine for near-IR photoimmunotherapy, *Dyes Pigm.*, 2023, **212**, 111101.
91 S. Alimohammadvand, M. K. Zenjanab, M. Mashinchian, J. Shayegh and R. Jahanban-Esfahlan, Recent advances in biomimetic cell membrane-camouflaged nanoparticles for cancer therapy, *Biomed. Pharmacother.*, 2024, **177**, 116951.
92 L. Hang, H. Li, M. Li, Y. Sun, W. Wu, L. Fang, Y. Diao, H. Qu, T. Zhang, S. Li and G. Jiang, Lactoferrin docking NIR-II cyanine dye as a potentiated phototheranostic for synchronous multimodal bioimaging and tumor photo-immunotherapy, *Theranostics*, 2024, **14**, 6671–6691.
93 J. Qiu, S. Gong, Y. Alp, J. Medeiros, E. Agnello and S. Thayumanavan, Membrane Fusion Drives Facile Uptake of Cell Membrane-Coated Nanocarriers, *ACS Nano*, 2025, **19**, 23001–23010.
94 N. Khosravi, E. Pishavar, B. Baradaran, F. Oroojalian and A. Mokhtarzadeh, Stem cell membrane, stem cell-derived exosomes and hybrid stem cell camouflaged nanoparticles: A promising biomimetic nanoplatforms for cancer theranostics, *J. Controlled Release*, 2022, **348**, 706–722.
95 Y. Zhuo, Z. Luo, Z. Zhu, J. Wang, X. Li, Z. Zhang, C. Guo, B. Wang, D. Nie, Y. Gan, G. Hu and M. Yu, Direct cytosolic delivery of siRNA via cell membrane fusion using cholesterol-enriched exosomes, *Nat. Nanotechnol.*, 2024, **19**, 1858–1868.
96 Y. Li, C. Zhang, Q. Wu, Y. Peng, Y. Ding, Z. Zhang, X. Xu and H. Xie, Enzyme-Activatable Near-Infrared Photosensitizer with High Enrichment in Tumor Cells Based on a Multi-Effect Design, *Angew. Chem., Int. Ed.*, 2024, **63**, e202317773.
97 R. Wang, X. Xia, Y. Yang, X. Rong, T. Liu, Z. Su, X. Zeng, J. Du, J. Fan, W. Sun and X. Peng, A Glutathione Activatable Photosensitizer for Combined Photodynamic and Gas Therapy under Red Light Irradiation, *Adv. Healthcare Mater.*, 2022, **11**, 2102017.
98 Q. Zeng, X. Li, J. Li, M. Shi, Y. Yao, L. Guo, N. Zhi and T. Zhang, Totally Caged Type I Pro-Photosensitizer for Oxygen-Independent Synergistic Phototherapy of Hypoxic Tumors, *Adv. Sci.*, 2024, **11**, 2400462.
99 J. Han, M. Yang, K. Li, W. Liu, J. Fan and X. Peng, A Universal Single-Activated-Dual-Release Vehicle: Enabling Synergistic Antitumor Therapy, *Small*, 2025, **21**, 2410925.
100 Y. Zhang, C. Yan, Q. Zheng, Q. Jia, Z. Wang, P. Shi and Z. Guo, Harnessing Hypoxia-Dependent Cyanine Photocages for *In Vivo* Precision Drug Release, *Angew. Chem., Int. Ed.*, 2021, **60**, 9553–9561.
101 H. Huang, Q. S. Tong, Y. Chen, X. Y. Liu, R. Liu, S. Shen, J. Z. Du and J. Wang, PAMAM-Based Polymeric Immunogenic Cell Death Inducer To Potentiate Cancer Immunotherapy, *J. Am. Chem. Soc.*, 2024, **146**, 29189–29198.
102 Y. Wu, K. Wei, G. Ma, C. Ji and M. Yin, A heptamethine cyanine with *meso*-N-induced rearrangement for acid-activated tumour imaging and photothermal therapy, *Biomater. Sci.*, 2022, **10**, 2964–2971.
103 W. Li, J. Huang, C. Shen, W. Jiang, X. Yang, J. Huang, Y. Gu, Z. Li, Y. Ma and J. Bian, Tumor-targeted metabolic inhibitor prodrug labelled with cyanine dyes enhances immunoprevention of lung cancer, *Acta Pharm. Sin. B.*, 2024, **14**, 751–764.
104 S. Diao, Z. Zhang, S. Zhao, Q. Li, X. Zhang, X. Yang, Z. Xu, M. Liu, W. Zhou, R. Li, C. Xie and Q. Fan, Dual-Activatable Nano-Immunomodulator for NIR-II Fluorescence Imaging-Guided Precision Cancer Photodynamic Immunotherapy, *Adv. Sci.*, 2024, **11**, 2409833.
105 L. Chen, J. Yang, F. Su, Z. Liu, S. Huang, J. Zhang, J. Li and W. Mao, A novel cyanine photosensitizer for sequential dual-site GSH depletion and ROS-potentiated cancer photodynamic therapy, *Eur. J. Med. Chem.*, 2025, **283**, 117165.
106 D. Fu, Y. Wang, K. Lin, L. Huang, J. Xu and H. Wu, Engineering of a GSH activatable photosensitizer for enhanced photodynamic therapy through disrupting redox homeostasis, *RSC Adv.*, 2023, **13**, 22367–22374.
107 C. Y. Chen, C. B. Jian, H. D. Gao, X. E. Yu, Y. C. Chang, S. K. Leong, J. J. Shie and H. M. Lee, Active loading of cyanine 5.5 derivatives into liposomes for deep self-quenching and their applications in deep tissue imaging, *Sens. Diagn.*, 2024, **3**, 1028–1038.
108 D. H. Li, R. S. Gamage, A. G. Oliver, N. L. Patel, S. Muhammad Usama, J. D. Kalen, M. J. Schnermann and B. D. Smith, Doubly Strapped Zwitterionic NIR-I and NIR-II Heptamethine Cyanine Dyes for Bioconjugation and Fluorescence Imaging, *Angew. Chem., Int. Ed.*, 2023, **62**, e202305062.
109 X. Zhao, Y. Yang, Y. Yu, S. Guo, W. Wang and S. Zhu, A cyanine-derivative photosensitizer with enhanced photostability for mitochondria-targeted photodynamic therapy, *Chem. Commun.*, 2019, **55**, 13542–13545.

110 T. Chen, Y. Zheng, Y. Gao and H. Chen, Photostability investigation of a near-infrared-II heptamethine cyanine dye, *Bioorg. Chem.*, 2022, **126**, 105903.
111 D. H. Li, R. S. Gamage and B. D. Smith, Sterically Shielded Hydrophilic Analogs of Indocyanine Green, *J. Org. Chem.*, 2022, **87**, 11593–11601.
112 D. H. Li and B. D. Smith, Supramolecular Mitigation of the Cyanine Limit Problem, *J. Org. Chem.*, 2022, **87**, 5893–5903.
113 R. S. Gamage, D. H. Li, C. L. Schreiber and B. D. Smith, Comparison of cRGDfK Peptide Probes with Appended Shielded Heptamethine Cyanine Dye (s775z) for Near Infrared Fluorescence Imaging of Cancer, *ACS Omega*, 2021, **6**, 30130–30139.
114 S. Yang, Y. Diao, L. Hang, H. Qu, L. Fang, W. Guo, H. Wen, K. Iu, G. Jiang, L. Shao and Q. Li, BSA@IR780-loaded mesoporous polydopamine nanoparticles with enhanced photostability for multimodal imaging and photothermal therapy of tumors, *Nanoscale Adv.*, 2025, **7**, 2182–2194.
115 Y. Li, T. Ma, H. Jiang, W. Li, D. Tian, J. Zhu and Z. Li, Anionic Cyanine J-Type Aggregate Nanoparticles with Enhanced Photosensitization for Mitochondria-Targeting Tumor Phototherapy, *Angew. Chem., Int. Ed.*, 2022, **61**, e202203093.
116 P. Kumari, S. Arora, Y. Pan, I. Ahmed, S. Kumar and B. Parshad, Tailoring Indocyanine Green J-Aggregates for Imaging, Cancer Phototherapy, and Drug Delivery: A Review, *ACS Appl. Bio Mater.*, 2024, **7**, 5121–5135.
117 H. Huang, Y. Wu, X. He, Y. Liu, J. H. Zhu, M. Gu, D. Zhou, S. Long, Y. Chen, L. Wang, M. Li, X. Chen and X. Peng, Electrostatic Co-Assembly of Cyanine Pair for Augmented Photoacoustic Imaging and Photothermal Therapy, *Adv. Sci.*, 2025, **12**, 2416905.
118 C. Teng, H. Dang, Y. Xu, D. Yin and L. Yan, Antiaggregation of NIR-II Probe Regulated by Amphiphilic Polypeptide with High Contrast Brightness for Phototheranostics and Vascular Microscopic Imaging under 1064 nm Irradiation, *Adv. Healthcare Mater.*, 2023, **12**, 2300541.
119 X. Hu, C. Zhu, F. Sun, Z. Chen, J. Zou, X. Chen and Z. Yang, J-Aggregation Strategy toward Potentiated NIR-II Fluorescence Bioimaging of Molecular Fluorophores, *Adv. Mater.*, 2024, **36**, 2304848.
120 J. Xu, X. Zheng, T.-B. Ren, L. Shi, X. Yin, L. Yuan and X. B. Zhang, Recent advances in near-infrared-II organic J-aggregates for bio-applications, *Coord. Chem. Rev.*, 2025, **528**, 216379.
121 J. Yu, J. Rong, S. Yuan, X. He, X. Chu, L. Chen, Q. Liu, S. Hu and Z. Wang, Extending the emission peak tail of indole cyanine for deep-near-infrared bioimaging, *Spectrochim. Acta, Part A Mol. Biomol. Spectrosc.*, 2024, **322**, 124798.
122 Y.-F. Ou, H.-Y. Xiang, X. Yang, R.-X. Wang, S.-Y. Huan, L. Yuan, T.-B. Ren and X.-B. Zhang, Constructing Stable and Wavelength-Extended Heptamethine Cyanines via Donor Ectopic Substitution for NIR-IIa/b Bioimaging, *Angew. Chem., Int. Ed.*, 2025, **64**, e202423978.
123 S. Lei, F. Zhao, J. Zhang, N. T. Blum, T. He, J. Qu, P. Huang and J. Lin, Metallo-Dye-Based Supramolecular Nanoassembly for NIR-II Cancer Theranostics, *Anal. Chem.*, 2022, **94**, 8399–8408.
124 J. Zhu, Y. Jiang, X. Pan, K. Xu, W. Niu, Y. Lv, C. Li, Y. Wang, Z. Xue, P. Lei and Y. He, *In Vivo* Evaluation of a Gallium-68-Labeled Tumor-Tracking Cyanine Dye for Positron Emission Tomography/Near-Infrared Fluorescence Carcinoma Imaging, Image-Guided Surgery, and Photothermal Therapy, *ACS Omega*, 2023, **8**, 6067–6077.
125 C. Guo, F. Li, S. Wu, C. Li, T. Hou, G. Li, J. Guo, X. Wang, L. Hao and Z. Li, Self-Assembled Gd/Cyanine Nanoplatform for Magnetic Resonance Imaging Guided Photothermal Therapy of Thyroid Cancer, *ACS Appl. Nano Mater.*, 2025, **8**, 6604–6614.
126 X. Mu, F. Wu, Y. Tang, R. Wang, Y. Li, K. Li, C. Li, Y. Lu, X. Zhou and Z. Li, Boost photothermal theranostics via self-assembly-induced crystallization (SAIC), *Aggregate*, 2022, **3**, e170.
127 K. Wei, Y. Wu, P. Li, X. Zheng, C. Ji and M. Yin, Modulating planarity of cyanine dye to construct highly stable H-aggregates for enhanced photothermal therapy, *Nano Res.*, 2022, **16**, 970–979.
128 X. Zou, Y. Zhao and W. Lin, Photoacoustic/fluorescence dual-modality cyanine-based probe for real-time imaging of endogenous cysteine and in situ diagnosis of cervical cancer *in vivo*, *Anal. Chim. Acta*, 2023, **1239**, 340713.
129 X. Hao, M. Gao, R. Zhang, Y. Tang, X. Mu, Y. Zhao, Y. Lu and X. Zhou, Synergistic Phototherapy Using Zwitterionic Crystalline Nanoaggregates of Orthogonal Donor-Acceptor Small-Molecule Dyads, *Adv. Funct. Mater.*, 2024, **35**, 2416317.
130 B. Huang, X. Liu, G. Yang, J. Tian, Z. Liu, Y. Zhu, X. Li, G. Yin, W. Zheng, L. Xu and W. Zhang, A Near-Infrared Organoplatinum(II) Metallacycle Conjugated with Heptamethine Cyanine for Trimodal Cancer Therapy, *CCS Chem.*, 2022, **4**, 2090–2101.
131 Z. Zhou, X. Jiang, L. Yi, C. Li, H. Wang, W. Xiong, Z. Li and J. Shen, Mitochondria Energy Metabolism Depression as Novel Adjuvant to Sensitize Radiotherapy and Inhibit Radiation Induced-Pulmonary Fibrosis, *Adv. Sci.*, 2024, **11**, 2401394.
132 M. Gao, X. Huang, Z. Wu, W. Xiao, Z. Du, B. Mo, C. Wu, H. Xing, W. Wang, R. Li and S. Luo, Albumin tailoring molecular rotation and electrophilicity of a GSH-depleting radiosensitizer for potentiating ferroptosis-mediated radioimmunotherapy, *Chem. Eng. J.*, 2024, **495**, 153595.
133 Z. Zhou, C. Li, C. Li, L. Zhou, S. Tan, W. Hou, C. Xie, L. Wang, J. Shen and W. Xiong, Mitochondria-Targeted Nanoadjuvants Induced Multi-Functional Immune-Microenvironment Remodeling to Sensitize Tumor Radio-Immunotherapy, *Adv. Sci.*, 2024, **11**, 2400297.
134 L. Fu, Y. Huang, X. Shan, X. Sun, X. Wang, X. Wang, L. Chen and S. Yu, NIR-activatable nitric oxide generator based on nanoparticles loaded small-molecule photosensitizers for synergetic photodynamic/gas therapy, *J. Nanobiotechnol.*, 2024, **22**, 595.
135 H. Kong, Y. Tang, X. Hao, W. Feng, W. Jiang, X. Mu, X. Jing, Y. Lu and X. Zhou, Self-Assembly of H_2S-Generating

Photosensitizer for Gas-Assisted Synergistic Photothermal Therapy, *Small*, 2025, **21**, 2411242.

136 K. Wei, Y. Wu, X. Zheng, L. Ouyang, G. Ma, C. Ji and M. Yin, A Light-Triggered J-Aggregation-Regulated Therapy Conversion: from Photodynamic/Photothermal Therapy to Long-Lasting Chemodynamic Therapy for Effective Tumor Ablation, *Angew. Chem., Int. Ed.*, 2024, **63**, e202404395.

137 Y. Zou, W. Liu, W. Sun, J. Du, J. Fan and X. Peng, Highly Inoxidizable Heptamethine Cyanine–Glucose Oxidase Conjugate Nanoagent for Combination of Enhanced Photothermal Therapy and Tumor Starvation, *Adv. Funct. Mater.*, 2022, **32**, 2111853.

138 Z. Hu, R. Li, X. Cui, C. Hu and Z. Chen, A pH-sensitive carbonic anhydrase IX-targeted near-infrared probe for fluorescent sensing and imaging of hypoxic osteosarcoma, *Sens. Actuators, B*, 2023, **379**, 133171.

139 J. Yan, H. Wang, X. Zhao, L. Tao, X. Wang and J. Yin, Polymorphic Supramolecular Therapeutic Platforms with Precise Dye/Drug Ratio to Perform Synergistic Chemo-Photo Anti-Tumor Therapy and Long-Term Immune Protection, *Adv. Healthcare Mater.*, 2024, **13**, 2402907.

140 Y. Park, J. Yang, M. S. Kim and H. Hyun, A Three-In-One Heptamethine Cyanine Dye Induces Endoplasmic Reticulum Stress and Apoptosis in Colorectal Cancer, *Adv. Healthcare Mater.*, 2025, **14**, 2404027.

141 C. Teng, Y. Xu, Y. Wang, D. Chen, D. Yin and L. Yan, J-aggregates of multi-groups cyanine dye for NIR-IIa fluorescence-guided mild photothermal therapy under 1064 nm irradiation, *J. Colloid Interface Sci.*, 2024, **670**, 751–761.

142 P. Muangsopa, K. Chansaenpak, S. Kampaengsri, J. Saetiew, P. Noisa, P. Meemon and A. Kamkaew, Hybrid Cyanine/Methotrexate Nanoparticles for Synergistic PDT/Chemotherapy of Breast Cancer, *ACS Appl. Bio Mater.*, 2023, **6**, 603–614.

143 M. Zheng, J. Zhang, C. Deng, L. Chen, H. Zhang, J. Xin, O. Aras, M. Zhou, F. An and Y. Ren, The collaborated assembly of hydrophobic curcumin and hydrophilic cyanine dye into nanocolloid for synergistic chemo-photothermal cancer therapy, *Mater. Des.*, 2024, **241**, 112900.

144 J. Zhu, A. Ouyang, J. He, J. Xie, S. Banerjee, Q. Zhang and P. Zhang, An ultrasound activated cyanine-rhenium(I) complex for sonodynamic and gas synergistic therapy, *Chem. Commun.*, 2022, **58**, 3314–3317.

145 X. Guan, N. Zeng, Y. Zhao, X. Huang, S. Lai, G. Shen, W. Zhang, N. Wang, W. Yao, Y. Guo, R. Yang, Z. Wang and X. Jiang, Dual-Modality Imaging-Guided Manganese-Based Nanotransformer for Enhanced Gas-Photothermal Therapy Combined Immunotherapeutic Strategy Against Triple-Negative Breast Cancer, *Small*, 2024, **20**, 2307961.

146 X. Luo, T. Zhao, S. Qin, F. Wang, J. Ran, Y. Hu and W. Han, Multifunctional metal-organic frameworks with photothermal-triggered nitric oxide release for gas/photothermal synergistic cancer therapy, *J. Colloid Interface Sci.*, 2025, **684**, 47–59.

147 Y. Yu, H. Wang, Z. Zhuang, C. Ji, L. Zhang, Y. Li, Z. Zhao, D. Ding, G. Feng and B. Z. Tang, Self-Adaptive Photodynamic-to-Photothermal Switch for Smart Antitumor Photoimmunotherapy, *ACS Nano*, 2024, **18**, 13019–13034.

148 H. Yang, F. Li, S. Jin, S. Chen, L. Sun, L. Wei, G. Xu, S. Cao, W. Song, X. Zeng, W. Zhong and W. Sun, An antioxidative-enhanced endoplasmic reticulum-targeted cyanine dye for efficient tumor immunotherapy, *Chem. Eng. J.*, 2024, **494**, 153089.

149 X. Huang, M. Gao, H. Xing, Z. Du, Z. Wu, J. Liu, T. Li, J. Cao, X. Yang, R. Li, W. Wang, J. Wang and S. Luo, Rationally Designed Heptamethine Cyanine Photosensitizers that Amplify Tumor-Specific Endoplasmic Reticulum Stress and Boost Antitumor Immunity, *Small*, 2022, **18**, 2202728.

150 Y. Qin, G. Wang, L. Chen, Y. Sun, J. Yang, Y. Piao, Y. Shen and Z. Zhou, High-Throughput Screening of Surface Engineered Cyanine Nanodots for Active Transport of Therapeutic Antibodies into Solid Tumor, *Adv. Mater.*, 2024, **36**, 2302292.

151 X. Jiang, L. Yi, C. Li, H. Wang, W. Xiong, Y. Li, Z. Zhou and J. Shen, Mitochondrial Disruption Nanosystem Simultaneously Depressed Programmed Death Ligand-1 and Transforming Growth Factor-beta to Overcome Photodynamic Immunotherapy Resistance, *ACS Nano*, 2024, **18**, 3331–3348.

152 S. Kwiatkowski, B. Knap, D. Przystupski, J. Saczko, E. Kędzierska, K. Knap-Czop, J. Kotlińska, O. Michel, K. Kotowski and J. Kulbacka, Photodynamic therapy-mechanisms, photosensitizers and combinations, *Biomed. Pharmacother.*, 2018, **106**, 1098–1107.

153 W. Zhao, L. Wang, M. Zhang, Z. Liu, C. Wu, X. Pan, Z. Huang, C. Lu and G. Quan, Photodynamic therapy for cancer: mechanisms, photosensitizers, nanocarriers, and clinical studies, *MedComm*, 2024, **5**, e603.

154 X. Deng, Z. Shao and Y. Zhao, Solutions to the Drawbacks of Photothermal and Photodynamic Cancer Therapy, *Adv. Sci.*, 2021, **8**, 2002504.

155 M. Kozlikova, M. A. Alfred, M. Machacek, F. Dumoulin, A. d. Escosura, T. Goslinski, M. Halaskova, J. D. Huang, M. R. Ke, S. Makhseed, D. T. Mlynarczyk, D. K. P. Ng, T. Torres, R. C. H. Wong, P. Zimcik and V. Novakova, Identifying Structural Factors Governing the Photodynamic Activity of Phthalocyanines, Identifying Structural Factors Governing the Photodynamic Activity of Phthalocyanines, *J. Med. Chem.*, 2026, **69**, 4391–4407.

156 D. Chen, Q. Xu, W. Wang, J. Shao, W. Huang and X. Dong, Type I Photosensitizers Revitalizing Photodynamic Oncotherapy, *Small*, 2021, **17**, 2006742.

157 S. Li, X. Jin, Z. Zhang, J. Li and J. Hua, An AIE-active type I photosensitizer based on N, N0-diphenyl-dihydrophenazine for high-performance photodynamic therapy under hypoxia, *Mater. Chem. Front.*, 2023, **7**, 3738–3746.

158 G. Sini, M. Schubert, C. Risko, S. Roland, O. P. Lee, Z. Chen, T. V. Richter, D. Dolfen, V. Coropceanu, S. Ludwigs, U. Scherf, A. Facchetti, J. M. J. Fréchet and D. Neher, On

the Molecular Origin of Charge Separation at the Donor-Acceptor Interface, *Adv. Energy Mater.*, 2018, **8**, 1702232.

159 X. Zhao, S. He, J. Wang, J. Ding, S. Zong, G. Li, W. Sun, J. Du, J. Fan and X. Peng, Near-Infrared Self-Assembled Hydroxyl Radical Generator Based on Photoinduced Cascade Electron Transfer for Hypoxic Tumor Phototherapy, *Adv. Mater.*, 2023, **35**, 2305163.

160 F. Han, M. Guo, X. Zhou, Z. Zhang, H. Zhang, L. Cai, X. Li, T. Shi, S. Long, W. Sun, J. Du, J. Fan and X. Peng, Precise Molecular Engineering of Heptamethine Cyanine-Based Near-Infrared Type-I Photosensitizers for Pro-Death Autophagy and Hypoxia-Tolerant Antitumor Treatment, *Angew. Chem., Int. Ed.*, 2025, **64**, e202504227.

161 Y. Shimoda, K. Miyata, M. Funaki, T. Ehara, T. Morimoto, S. Nozawa, S. Adachi, O. Ishitani and K. Onda, Determining Excited-State Structures and Photophysical Properties in Phenylphosphine Rhenium(I) Diimine Biscarbonyl Complexes Using Time-Resolved Infrared and X-ray Absorption Spectroscopies, *Inorg. Chem.*, 2021, **60**, 7773–7784.